SEISMIC HAZARD ZONE REPORT 134

SEISMIC HAZARD ZONE REPORT FOR THE RICHMOND, MARE ISLAND, AND SAN QUENTIN 7.5-MINUTE QUADRANGLES, CONTRA COSTA COUNTY, CALIFORNIA

2024

STATE OF CALIFORNIA
GAVIN NEWSOM
GOVERNOR

THE RESOURCES AGENCY
WADE CROWFOOT
SECRETARY FOR RESOURCES

DEPARTMENT OF CONSERVATION
DAVID SHABAZIAN
DIRECTOR

CALIFORNIA GEOLOGICAL SURVEY
JEREMY LANCASTER
STATE GEOLOGIST

CALIFORNIA GEOLOGICAL SURVEY
JEREMY LANCASTER, STATE GEOLOGIST

Web Accessibility Statement: If you find any part of this document to be inaccessible with assistive technology, visit our Accessibility web page at conservation.ca.gov to report the issue and request alternative means of access. To help us respond to your concern, please include the following three items in your request: 1. your contact information. 2. the title of this document. 3. the web address where you obtained the document.

Release and Revision History: Seismic Hazard Zone Map and Evaluation Report of the Richmond, Mare Island, and San Quentin Quadrangles, Contra Costa County, SHZR 134	
August 24, 2023	Preliminary Map Release
February 22, 2024	Official Map Release

TABLE OF CONTENTS

TABLES

PLATES

EXECUTIVE SUMMARY

This report summarizes the sources of information and methods used to prepare the map of *Seismic Hazard Zones* (a subset of *Earthquake Zones of Required Investigation* (EZRI)) for the Richmond, Mare Island, and San Quentin 7.5-Minute quadrangles, Contra Costa County, California. The topographic quadrangle maps, which cover approximately 190 square kilometers (~74 square miles) at a scale of 1:24,000 (41.7 mm = 1,000 meters; 1 inch = 2,000 feet), displays the boundaries of the EZRI for liquefaction and earthquake-induced landslides. The area subject to seismic hazard mapping includes the cities of Richmond, El Cerrito, Pinole, San Pablo, Hercules, and the unincorporated census designated places of Kensington, East Richmond Heights, North Richmond, Rollingwood, El Sobrante, Montalvin Manor, Bayview, Tara Hills, Luzon, and Rodeo.

This Seismic Hazard Zone Report describes the development of the Seismic Hazard Zone for the Richmond, Mare Island, and San Quentin 7.5-Minute quadrangles. The process of zonation for liquefaction hazard involves evaluation of earthquake loading, Quaternary geologic maps, groundwater level records, and subsurface geotechnical data. The process of zonation for earthquake-induced landslide hazard incorporates evaluation of earthquake loading, existing landslides, slope gradient, rock strength, and geologic structure. Ground motion calculations used by CGS exclusively for regional zonation assessments are currently based on the probabilistic seismic hazard analysis (PSHA) model developed by the United States Geological Survey for the 2018 *Update of the United States National Seismic Hazard Maps*.

About 58 square kilometers (22 square miles) of land in Contra Costa County in the Richmond, Mare Island, and San Quentin quadrangles (project area) has been designated EZRI for liquefaction hazard, encompassing much of the East Bay alluvial plain, Wildcat Creek, San Pablo Creek, Pinole Creek alluvial valleys, and smaller unnamed valleys and canyons dissecting the hills southeast of Pinole and El Sobrante and northeast of Richmond. Borehole logs of test holes drilled in these areas indicate the widespread presence of near-surface soil layers composed of saturated, loose sandy sediments. Geotechnical tests conducted downhole and in labs indicate that these soils generally have a moderate to high likelihood of liquefying, given the level of strong ground motions this region could be subjected to.

About 22 square kilometers (9 square miles) of land in the project area has been designated EZRI for earthquake-induced landslides, encompassing much of the East Bay Hills and including the moderate to steep slopes of Pinole Ridge, El Sobrante Ridge, San Pablo Ridge, hills around Point Richmond and Point San Pablo, and the Berkeley Hills, as well as minor unnamed terrain throughout the map area.

City, county, and state agencies are required by the California Seismic Hazards Mapping Act to use the Seismic Hazard Zone maps in their land-use planning and permitting processes. They must withhold building permits for sites being developed within EZRI until the geologic and soil conditions of the project site are investigated and appropriate mitigation measures, if any, are incorporated into development plans. The Act also requires sellers of real property within these zones to disclose that fact at the time such property is sold.

INTRODUCTION

The California Seismic Hazards Mapping Program

The Seismic Hazards Mapping Act of 1990 (the Act) (Public Resources Code, Division 2, Chapter 7.8) directs the State Geologist to prepare maps that delineate Seismic Hazard Zones for liquefaction, earthquake-induced landslides, tsunami inundation, and other ground failures. These are a subset of Earthquake Zones of Required Investigation (EZRI), which also include Earthquake Fault Zones. The California Geological Survey (CGS) prepares EZRI following guidelines prepared by the California State Mining and Geology Board (SMGB). For liquefaction and landslide hazard zone delineation, the SMGB established the Seismic Hazard Mapping Act Advisory Committee to develop guidelines and criteria for the preparation of seismic hazard zones in the state. The committee's recommendations are published in CGS Special Publication 118, which is available on online at: http://www.conservation.ca.gov/cgs/publications/sp118.

The purpose of the Act is to reduce the threat to public health and safety by identifying and mitigating seismic hazards. City, county, and state agencies are directed to use the Seismic Hazard Zone maps in their land-use planning and permitting processes. They must withhold development permits for a site within a zone until the geologic and soil conditions of the project site are investigated and appropriate mitigation measures, if any, are incorporated into development plans. The Act also requires sellers (and their agents) of real property within a mapped hazard zone to disclose at the time of sale that the property lies within such a zone. State-of-the-practice evaluation and mitigation of seismic hazards are conducted under guidelines published in CGS Special Publication 117A, which are available online at: http://www.conservation.ca.gov/cgs/publications/sp117a.

Following the initial release of the Special Publication 117 in 1997, local government agencies in the Los Angeles metropolitan region sought more definitive guidance in the review of geotechnical investigations addressing liquefaction and landslide hazards. These agencies convened two independent committees, one for liquefaction and one for landslides, to provide more detailed procedures for implementing Special Publication 117 guidelines. The reports produced by these committees were published under the auspices of the Southern California Earthquake Center (SCEC) and are available online at: http://www-scec.usc.edu/resources/catalog/hazardmitigation.html. Special Publication 117 was revised in 2008 as Special Publication 117A.

Methodology and Organization of this Report

Delineating liquefaction and landslide hazard zones requires the collection, compilation, and analysis of multiple types of digital data. These data include geologic maps, ground water measurements, subsurface and laboratory geotechnical tests, elevation (terrain) maps, and probabilistic ground motion estimates. The data are processed into a series of geographic information system (GIS) layers using commercially available and open-source software, which are used as input for the delineation of hazard zones.

Earthquake Zones of Required Investigation (EZRI) for liquefaction and earthquake-induced landslides share many input datasets. Section 1 of this report describes the geographic, geologic, and hydrologic characteristics of the project area and laboratory tests used to categorize geologic materials within the quadrangle according to their susceptibility to liquefaction and/or landslide failure. Section 2 describes the development of the earthquake shaking parameters used in the liquefaction and landslide hazard analyses and summarizes the ground motions used to evaluate liquefaction and earthquake-induced landslide potential in the project area. Sections 3 and 4 summarize the analyses and criteria used to delineate liquefaction and earthquake-induced landslide hazard zones, respectively, in the project area.

Scope and Limitations

Seismic Hazard Zones for liquefaction and earthquake-induced landslides are intended to prompt more detailed, site-specific geotechnical investigations. Due to scale and other limitations inherent in these zones, they should not be used as a substitute for site-specific geologic or geotechnical investigations required under Chapters 7.5 and 7.8 of Division 2 of the California Public Resources Code. Site-specific geologic/geotechnical investigations are the best way to determine if these hazards could affect structures or facilities at a project site.

The zones described in this report identify areas where the potential for ground failure related to liquefaction and earthquake-induced landslides is relatively high. Liquefaction and landslides may occur outside the delineated zones in future earthquakes, but most of the occurrences should be within zoned areas. Conversely, not all the area within a hazard zone will experience damaging ground failure in future earthquakes. The analyses used to delineate liquefaction and earthquake-induced landslide zones cannot predict the amount or direction of liquefaction- or landslide-related ground displacements, or the amount of damage to structures or facilities that may result from such displacements. Because of this limitation, it is possible that run-out areas during future earthquakes could extend beyond zone boundaries.

Other earthquake-induced ground failures that are not specifically addressed in the analyses conducted for the project area include those associated with soft clay deformation, non-liquefaction-related settlement, ridge-top spreading, and shattered ridges.

Although data used in this evaluation was selected using rigorous criteria, the quality of the data used varies. The State of California and the Department of Conservation make no representations or warranties regarding the accuracy of the data obtained from outside sources.

Accessing Earthquake Zones of Required Investigation Maps, Reports, and GIS Data

CGS EZRI, including Seismic Hazard Zones and Earthquake Fault Zones, their related reports and GIS data, are available for download and/or online viewing on the CGS Information Warehouse: http://maps.conservation.ca.gov/cgs/informationwarehouse/.

Alternatively, EZRI are available as an interactive web map service (WMS) here: https://gis.conservation.ca.gov/server/rest/services/CGS_Earthquake_Hazard_Zones.

EZRI are also available on a statewide parcel base, which can be useful for initial Natural Hazards Disclosure determinations, by using the California Earthquake Hazards Zone Application (EQ Zapp): https://maps.conservation.ca.gov/cgs/EQZApp/app/.

Information on how to purchase EZRI maps and reports is available online at: http://www.conservation.ca.gov/cgs/publications.

Information regarding the Seismic Hazard Zonation Program is available on the CGS website: http://www.conservation.ca.gov/cgs/shzp/.

SECTION 1: GEOGRAPHY GEOLOGY AND ENGINEERING GEOLOGY

of the

RICHMOND, MARE ISLAND, AND SAN QUENTIN 7.5-MINUTE QUADRANGLES, CONTRA COSTA COUNTY, CALIFORNIA

by

Jacqueline Bott
P.G. 7459 C.E.G. 2382

DEPARTMENT OF CONSERVATION
CALIFORNIA GEOLOGICAL SURVEY

Purpose of this Section

Preparing Earthquake Zones of Required Investigation (EZRI) for liquefaction and earthquake-induced landslides requires many input datasets and complex analyses. The purpose of Section 1 of the Seismic Hazard Zone Report is to describe the overall geologic and geographic setting of the Richmond, Mare Island, and San Quentin quadrangles (the project area) and then discuss the collection, processing, and analyses of primary geologic and engineering geologic data that were used to delineate EZRI.

GEOGRAPHY

Location

The project area covers a region of approximately 266 square kilometers (103 square miles) in Contra Costa County, California. The center of the Richmond Quadrangle lies about 17 kilometers (11 miles) northeast of the City of San Francisco and about 100 kilometers (62.4 miles) southwest of the City of Sacramento. The map encompasses developed areas along the northern end of the East Bay Plain and adjoining East Bay Hills. It includes the cities of Richmond, San Pablo, El Cerrito, Pinole, and Hercules as well as the unincorporated census designated places of Kensington, East Richmond Heights, North Richmond, Rollingwood, El Sobrante, Tara Hills, Montalvin, Bayview, and Rodeo. The map also covers undeveloped and protected areas such as the Miller/Knox Regional Shoreline, Brooks Island Regional Preserve, Tilden Regional Park, Kennedy Grove Regional Park, Point Pinole Regional Shoreline, Pinole Valley Park, and smaller city parks.

The project area is located within the western California transpressional plate boundary. The dominant topographic feature in the project area is the East Bay Hills, which formed as part of a fold and thrust belt in the Coast Ranges Geomorphic Province. West of the East Bay Hills, alluvial fans have developed from outflow of San Pablo and Wildcat creeks, which are sourced within the East Bay Hills, out across the flat-lying plain southwest of the Hayward fault. The San Francisco Bay is located east of the Richmond and San Quentin quadrangles, and San Pablo Bay is located to the north of the land area in all three quadrangles within Contra Costa County. The highest point of the Richmond Quadrangle is 370 meters (1214 feet), located along the boundary between Contra Costa and Alameda counties in the east central portion of the quadrangle. The highest point in the San Quentin Quadrangle (in Contra Costa County) is just northwest of Point Richmond at 151 m (494 feet), and the highest point in the Mare Island Quadrangle (in Contra Costa County) is around 107 m (350 feet) towards the southeast corner of the quadrangle and south-southeast of the city of Hercules. The terrain changes abruptly along the southwest side of the Berkeley Hills along strike of the Hayward fault, with ridges and intervening valleys on the northeast side and the heavily populated southwest side developed on gently sloping piedmont and alluvial surfaces that extend down the San Francisco Bay. The East Bay Hills are eroded by seasonal and perennial creeks along northwest-southeast striking canyons (Wildcat Canyon, Pinole Creek canyon, and San Pablo Creek canyon).

To the north, within the Mare Island Quadrangle, the elevation and ruggedness slowly decrease northwestwards towards San Pablo Bay. Another steep-sided ridge occurs west of Richmond and the alluvial plain, extending along a northwest-southeast strike between Point Potrero at the southeastern tip and Point San Pablo on the northwestern tip. This ridge is parallel to the ridges in the East Bay Hills. The central portion of the ridge includes suburban development of Point Richmond, but north of the Knox Freeway (Interstate 580) is mostly industrial development such as Chevron refineries and other industry. The southern portion of the ridge is home to the Miller/Knox Regional Shoreline Park and some small suburban development around the Richmond Yacht Club and Boardwalk.

Land Use

The project area was initially inhabited by Ohlone Native Americans who settled here an estimated 5,000 years ago. The Ohlone were hunters and gatherers and built extensive shell mounds along the Bay. The homeland of the Muwekma Ohlone Tribe includes area now covered by the counties of San Francisco, San Mateo, most of Santa Clara, Alameda, Contra Costa, and portions of Napa, Santa Cruz, Solano, and San Joaquin. (https://cejce.berkeley.edu/ohloneland). Spanish colonizers arrived in 1772 and developed vast grain fields throughout the area.

Point Richmond was designated the western terminus of the Santa Fe Railroad in 1899 and the first passenger arrived in Richmond in 1900, travelling from Chicago. Shortly after, Standard Oil Company built its refinery in this area. The City of Richmond was incorporated in 1905 and became an industrial center. Construction of shipping port terminals began, and the Ford Motor Assembly plant was opened during the 1920's to 1930's. During World War II the Kaiser Richmond Shipyards became one of the biggest wartime shipbuilding operations along the west coast in 1941, and Richmond developed into a boomtown. Many of the tidal inlets in the area were filled to extend the land area at this time.

During the postwar period, the city of Richmond expanded by annexing land to the east, north and northwest. At this time the shipyards closed and were replaced by new industries, warehouses, and parts depots for Ford. Construction of the Knox Freeway and Richmond Parkway, along with the Marina Bay housing development and the Hilltop Shopping Center, transformed the economy in the 1960s. The urban centers of Hercules, Pinole, El Cerrito, and

San Pablo were incorporated in 1900, 1903, 1917, and 1948, respectively. The town of El Cerrito was a rural area in the 1900s but began to grow from refugees from the 1906 San Francisco earthquake and fire.

Large areas east of Kensington, El Cerrito, and Richmond are undeveloped and comprise the Wildcat Canyon Regional Park, Kennedy Grove Regional Recreation Area, and undeveloped lands of the East Bay Municipal Utility District surrounding the San Pablo and Briones reservoirs (the latter to the east of the Richmond Quadrangle).

The primary transportation routes in the map area consist of Interstate 80 that runs north and then northeastwards past Point Pinole, and Interstate 580 which separates from Interstate 80 just south of the boundary with Alameda County in the City of Albany. Interstate 580 then traverses north and then westward along the San Francisco Bay shoreline and then through the hills around Point Richmond, out to the San Rafael-Richmond Bridge which connects the east bay to San Rafael in Marin County. Interstate 80 provides a major route connecting the Bay Area with Sacramento to the northeast. Additional access is provided by a network of city, county, and private roads in the developed areas and by fire roads and trails in undeveloped areas.

Digital Terrain Data

A digital representation of the earth's surface is a key component in delineating liquefaction and earthquake-induced landslide hazards. Within the project area, digital topography in the form of a lidar-derived digital elevation model was obtained from the USGS (http://nationalmap.gov/elevation.html). These lidar data were collected in 2018 after several northern California wildfires, and present elevations at a point spacing of 1 meter, with 1-meter horizontal accuracy and 2-centimeter RMSE vertical accuracy. Lidar data collected by Contra Costa County in 2010 (https://gis.cccounty.us/Downloads/) were used for Brooks and Red Rock islands, as these areas were not included in the 2018 flightlines.

For liquefaction hazard analyses, surface elevations derived from the DEM are differenced with historic-high ground water elevations to derive a "depth to water" map. In alluvial areas, the depth value obtained is combined with geologic data from boreholes and used in liquefaction calculations.

For earthquake-induced landslide hazard analyses, slope gradient and slope aspect are calculated using the slope applications built into commercially available GIS software. Both parameters are calculated using a third-order, finite difference, center-weighted algorithm based on Horn (1981), as documented in Burrough and McDonnell (1998). The slope gradient is combined with the geologic material strength map to calculate yield acceleration, a measure of susceptibility to earthquake slope failure as described in Section 4 of this report. Slope aspect, the compass direction that a slope faces, is used to identify potential adverse geologic bedding conditions and refine the geologic material strength map.

GEOLOGY

The primary source of geologic information used in the evaluation of liquefaction and earthquake-induced landslide hazards in the project area is the bedrock geologic maps of

Graymer and others (1994), Graymer (2000), and newer mapping by Wagner and others (2021). The bedrock map compilation was combined with a geologic map compiled from Quaternary geologic mapping by Witter and others (2006), Knudsen and others (2000), and Graymer and others (1994)

Digital geologic maps covering the project area and adjacent areas were combined to form a single 1:24,000-scale geologic materials map. CGS staff used DEMs, aerial photos, online imagery, and limited field reconnaissance to modify the Quaternary/bedrock boundary, confirm the location of geologic contacts, map recently modified ground surfaces, observe properties of near-surface deposits, and characterize the surface expression of individual geologic units. Landslide deposits were deleted from the geologic map so that the distribution of bedrock formations and the newly created landslide inventory would exist on separate layers for the hazard analysis. Young alluvial valleys were added or modified by CGS geologists in some areas to refine the map and ensure continuity of geologic mapping with adjacent quadrangles. Linear structural features such as folds, faults, and anticlines that did not form a geologic boundary were removed. The distribution of Quaternary and bedrock deposits on the final geologic materials map was used, in combination with other data, to evaluate liquefaction and landslide susceptibility and develop the Seismic Hazard Zone Map.

The unit names and descriptions of bedrock deposits exposed in the study area are taken from Graymer and others (1994) and Wagner and others (2021). The Quaternary geologic unit nomenclature used by CGS for mapping in the San Francisco Bay Region was adopted from Witter and others (2006).

Bedrock Units

The bedrock geology of Contra Costa County has been divided by Graymer and others (1994) and Graymer (2000) into six individual fault-bounded stratigraphic assemblages (I – VI) representing separate depositional basins or different parts of large basins that were later juxtaposed by large offsets on strike-slip and dip-slip faults during Tertiary time. Stratigraphic Assemblages I, II, and III underly the project area and consist of lightly to highly deformed Mesozoic and folded and faulted Cenozoic rock complexes: The Franciscan Complex, the Jurassic Coast Range Ophiolite, and Tertiary Assemblages (Berkeley Hills, Briones Valley, Las Trampas Ridge, and El Sobrante), which lie unconformably on the Cretaceous Great Valley Sequence east of these quadrangles.

Mesozoic Rocks

Rocks of the Franciscan Complex (Jurassic to Upper Cretaceous) and Jurassic Coast Range Ophiolite are exposed along the southwest side of the East Bay Hills in Richmond and El Cerrito, south of where Wildcat Creek cuts through the hills in the Richmond Quadrangle and are separated from the Tertiary sedimentary and volcanic rocks to the northeast by a thrust fault. They also comprise some small hilly outcrops in the region of the Richmond Annex, just north of and along strike with Albany Hill, and are exposed on Brooks and Red Rocks islands and the hills near Point Richmond between Point Potrero and Point San Pablo. They represent an ancestral accretionary wedge of Jurassic oceanic crust and pelagic deposits overlain by Late Jurassic to Late Cretaceous turbidities. They consist of a mélange of metamorphic rocks, including glaucophane and other schistose rocks in a sheared sandstone and shale matrix (**KJfm**), small bodies of serpentinite matrix mélange and large blocks of high-grade metamorphic rocks such as amphibolite and actinolite schist (**spm**), and sandstone and metasandstone of the Novato Quarry (**Kfn**), Alcatraz (**Kfa**), and Yolla Bolly terranes (**KJfy**).

The Great Valley Sequence (Cretaceous and Jurassic) is exposed in the southeastern corner of the Richmond Quadrangle near the Alameda County boundary. It consists of highly altered intermediate and silicic volcanic and hypabyssal keratophyre and quartz keratophyre (**Jsv**) rocks that appear to be the altered remnants of the volcanic arc rocks overlying the ophiolite in the Jurassic Period (Graymer, 2000)

Cenozoic Units

Tertiary bedrock units rest unconformably on Mesozoic rocks and consist of a series of sandstone, conglomerate, and shale formations of Miocene age. They are exposed along northwest-trending banded outcrops forming similarly oriented ridges and valleys.

The Miocene rocks are divided into three stratigraphic groups which from the oldest to youngest are: the Monterey Group, the San Pablo Group, and the Contra Costa Group. The Monterey Group has marine containing foraminifera indicating deposition at bathyal depths. The San Pablo Group is comprised of dominantly shallow marine sediments but does contain some plants and mammal fossils indicative of terrestrial deposition. The Contra Costa Group is mostly continental and Wagner and others (2021) present new dates for the base of the earliest Contra Costa sediments at 12-11 Ma. Graham and others (1984) speculate that the change from marine to continental deposition through the Miocene resulted in a change from deposition in a subduction environment to a transform environment during the passage of the triple junction through this area.

New mapping by Wagner and others (2021) divides the Monterey Group into three sequences, of which the intermediate Monterey sequence outcrops in the Richmond Quadrangle and the eastern Monterey sequence outcrops in the northeastern portion of the Richmond Quadrangle and within the Mare Island Quadrangle. The third segment, the western Monterey sequence, outcrops south of the project area. The eastern Monterey sequence is primarily comprised of fine sandstones intercalated with thin shale beds, siliceous shales, and chert, such as the Hambre Sandstone (**Th),** Oursan Sandstone **(To)**, Rodeo Shale **(Tr),** Tice Shale **(Tt),** and Claremont Shale **(Tcs)**. The intermediate Monterey sequence contains sandstone (**Tsa**), conglomerate (**Tcgl**), siliceous shale (**Tmu**), and diatomite (**Tdi**). All three sequences are thought to be largely coeval based on dating of foraminifera.

Wagner and others (2021) newly define Garrity and Rodeo sections of the Contra Costa Group which outcrop in the Richmond and Mare Island quadrangles. The Garrity Formation (**Tgu, Tgl,** and **Tgud,** for upper member, lower member, and undifferentiated, respectively) previously mapped as Orinda Formation and unnamed sedimentary and volcanic rocks by Graymer and others (1994) and Graymer (2000), rests disconformably over the Monterey Group in the East Bay Hills. The Rodeo section and a transition zone between this and the Southern section (south of project area), both of which are located west of the Franklin fault, include sandstones of the Briones (**Tbr**), Cierbo (**Tc**), and Neroly formations (**Tn**) and the Hercules Shale member of the Briones Formation (**Tbh**). Also, at the top of this section the Roblar Tuff **(Tpcr),** dated at 6.2 Ma using ash correlations (Wagner and others, 2021), disconformably rests on the Neroly Sandstone.

Quaternary Sedimentary Deposits

Approximately 92.9 square kilometers (35.9 square miles) of the project area are covered by Quaternary sediments and historical artificial materials. In total, 25 different units are mapped in the project area (Plate 1.1). They are divided into groups based on age, origin, and composition (Table 1.1). The liquefaction susceptibility evaluation and development of the Seismic Hazard Zone Map for the quadrangles is based on the distribution of these deposits at a scale of 1:24,000 (Plate 1.1).

Pleistocene to Holocene alluvial sediments

Alluvial sediments occur along stream channels and adjoining flood prone areas in and at the mouth of Wildcat Canyon, San Pablo Creek valley, Pinole Valley, Refugio Valley, and other smaller valleys and canyons dissecting elevated terrain throughout the map area. These deposits include undifferentiated alluvium (**Qoa**, Early to Latest Pleistocene; **Qpa**, Latest Pleistocene; **Qa**, Latest Pleistocene to Holocene; **Qha**, Holocene), alluvial fans (**Qof**, Early to Latest Pleistocene; **Qpf**, Latest Pleistocene; **Qf**, Latest Pleistocene to Holocene; **Qhf**, Holocene; **Qhfy**, Latest Holocene), alluvial fan fine facies (**Qhff,** Latest Holocene), stream channel deposits (**Qhc**, Holocene), alluvial fan levee deposits (**Qhl**, Holocene; **Qhly**, Latest Holocene) stream terrace deposits (**Qht**, Holocene; **Qhty**, latest Holocene), estuarine San Francisco Bay Mud (**Qhbm**, Holocene), bay terrace (**Qbt**, Pleistocene), marine terrace (**Qmt**, Pleistocene), and pediment (**Qop**, Early to Latest Pleistocene). Alluvial sediments generally consist of poorly to moderately sorted, poorly to well bedded, loose to dense sand, gravel, silt, and clay. Pleistocene age is indicated by depth of stream incision, stronger soil development and lack of historical flooding evidence.

Historical artificial fills

Artificial undifferentiated fill (**af**) is material deposited by human activity and is found throughout the map area. Fill may be engineered or non-engineered material, both of which may occur within the same area on the map. An artificial channel (**ac**) is a concrete lined channel whereas artificial channel fill (**acf**) is material emplaced in a historically active stream channel to re-route water flow. Artificial dam fill (**adf**) is material emplaced to hold back water to create ponds and reservoirs, and artificial levee fill (**alf**) is material deposited to create an artificial levee along a stream or creek to prevent flooding. In some areas artificial fill has been emplaced directly over the San Francisco Bay mud (**afem**) to extend the land out into the bay.

Table 1.1. Quaternary units mapped in the Richmond, Mare Island, and San Quentin quadrangles.

Map Unit	Environment of Deposition	Age
ac	Artificial Stream Channel	Historical
acf	Artificial Channel Fill	Historical
adf	Artificial Dam Fill	Historical
af	Artificial Fill	Historical
afem	Artificial Fill over Estuarine Mud	Historical
alf	Artificial Levee Fill	Historical
Qhc	Stream Channel	Historical
Qhly	Alluvial Fan Levee	Latest Holocene
Qhty	Stream Terrace	Latest Holocene
Qhfy	Alluvial Fan	Latest Holocene
Qha	Undifferentiated Alluvium	Holocene
Qhf	Alluvial Fan	Holocene
Qht	Stream Terrace	Holocene
Qhl	Alluvial Fan Levee	Holocene
Qhff	Alluvial Fan, Fine Facies	Holocene
Qhbm	San Francisco Bay Estuarine Mud	Holocene
Qa	Undifferentiated Alluvium	Latest Pleistocene to Holocene
Qf	Alluvial Fan	Latest Pleistocene to Holocene
Qpa	Undifferentiated Alluvium	Latest Pleistocene
Qpf	Alluvial Fan	Latest Pleistocene
Qbt	Bay Terrace	Pleistocene
Qmt	Marine Terrace	Pleistocene
Qof	Alluvial Fan	Early to Late Pleistocene
Qoa	Undifferentiated Alluvium	Early to Late Pleistocene
Qop	Pediment	Early to Late Pleistocene

Geologic Structure

The structural framework of the project area is governed by the transform Pacific-North American plate boundary, which accommodates 4.8 centimeters of right-lateral plate motion per year (Petersen and others, 1996).

In the San Francisco Bay area, about three-fourths of this relative movement is accommodated by shearing distributed across a broad, complex belt marked by major northwest-trending faults, including the San Andreas, Hayward, and Calaveras, along with many parallel secondary faults such as the Greenville, Green Valley, and San Ramon-Concord. In the current transpressional tectonic regime, characterized by a horizontal northeast-southwest maximum compression direction, differential strike-slip movement along these faults locally generates fault propagation folds.

The East Bay Hills in the map area lie within a wide zone of dextral shear, cut by northwest trending dextral faults that produced both restraining and releasing structures due to several step overs (both right-stepping and left stepping), which influenced depositional centers and erosion during the Miocene with tectonically uplifted areas and spatially restricted sub-basins. Stratigraphic elements that differ across the region indicate that a small amount of post-10 Ma horizontal displacement has occurred as some clasts from the Monterey Group are found in the Orinda Formation nearby. Significant deformation occurred after deposition of the 6.2 Ma Roblar Tuff and overturned bedding has been observed at Rodeo, so folding is inferred as occurring after 6.2 Ma (Wagner and others, 2021). The Sobrante anticline is asymmetric, and beds are locally overturned. Folds in this area plunge steeply to the southeast. The Roblar Tuff is present in the Garrity Formation west of the West Pinole fault, and Wagner and others (2021) suggest significant post-6.2 Ma horizontal displacement as the thickness of tuff appears to differ significantly across the fault.

Several Quaternary faults cross the project area. The northwest trending right-lateral strike-slip Hayward fault marks the western border of the East Bay Hills. It is identified by geomorphic and tonal features in Holocene alluvium and is considered well-defined in the project area, except in areas of Franciscan bedrock and areas of mass wasting on the west side of the East Bay Hills. As such, it is included in an Alquist-Priolo Fault Zone. The location of the Hayward fault is not well-constrained in San Pablo Bay, although it is thought to connect under the bay with the Rodgers Creek fault in Sonoma County. The Pinole fault to the east of the Hayward fault is thought to be connected to another branch of the Rodgers Creek fault that also connects under San Pablo Bay, but these are not considered Holocene-active structures.

Adverse Bedding Conditions

Adverse bedding conditions are an important consideration in slope stability analyses. Adverse bedding conditions occur where the dip direction of bedded sedimentary rocks is roughly the same as the slope aspect, and where the dip magnitude is less than the slope gradient. Under these conditions, landslides can slip along bedding surfaces due to a lack of lateral support. To account for adverse bedding in our slope stability evaluation, we used geologic structural data in combination with digital terrain data to identify areas with potentially adverse bedding, using methods like those of Brabb (1983). The structural data, strike and dip measurements, and fold axes derived from the geologic map database were used to categorize areas of common bedding dip direction and magnitude. The dip direction was then compared to the slope aspect and, if the same, the dip magnitude and slope gradient categories were compared. The area was marked as a potential adverse bedding area if the dip magnitude category was less than or equal to the slope gradient category, but greater than 25% (4:1 slope).

Existing Landslides

As a part of the geologic data compilation, an inventory of existing landslides in the project area has been prepared primarily from geomorphic analyses of lidar-derived elevation data and Google Earth Pro imagery as well as through field reconnaissance and review of previously published (Bishop and others, 1973) and unpublished landslide mapping. The lidar dataset consists of 1.0-meter bare earth DEM derived hillshade, contour, slope, and other derivative layers. These data were acquired by Contra Costa County in 2010 and the USGS in 2018 and meet QL2 accuracy with 4 points and 2 points per meter pulse density, respectively. All landslides in this inventory were digitized in an ArcGIS environment at a resolution of no larger than 1:2,000.

For each landslide included on the map, several characteristics (attributes) were compiled. These characteristics include the confidence of interpretation (definite, probable, or questionable), activity, thickness, and associated geologic unit(s). The completed landslide map was digitized, and the attributes were entered into a database. Landslides rated as definite, or probable were carried into the landslide zone as described in Section 4. A small-scale version of this landslide inventory is included on Plate 1.2 for the project area.

A total of 492 landslides were mapped in the project area, of which the majority (480) occurred within the Richmond Quadrangle. There are 238 rock slides, 139 earth flows, 75 debris slides, 25 debris flows, 10 debris fans, three soil slides, and two uncertain slides. These landslides have mostly developed on moderate to steep slopes of the Berkeley Hills, San Pablo Ridge, Sobrante Ridge, Pinole Ridge, and minor unnamed terrain throughout the map area.

The largest amount of land covered by landslides occurs mainly in the youngest Miocene sedimentary Garrity Formation (**Tgud, Tgl,** and **Tgu**, 79%), followed by the Franciscan Complex mélange, sandstones and serpentinite (**KJfm, Kfn, KJfy, KJm, spm,** 20%). In terms of area percentage affected by landslides, the bedrock geologic units most susceptible to landsliding are the Pliocene and Miocene conglomerate, sandstone and siltstone (**Tcgl**, 87%), Franciscan Alcatraz Terrane sandstone (**Kfa**, ~50%), Franciscan Complex Yolla Bolly metasandstone (**KJfy**, 43%), Franciscan Complex mélange (**KJfm,** 36%), serpentinite (**spm**, 32%), Hambre Sandstone (**Th**, 25%), Garrity Formation (**Tgud, Tgl and Tgu,** 18%), and Oursan Sandstone (**To**, 13%).

Historic-High Groundwater Mapping

Liquefaction occurs only in saturated soil conditions, and the susceptibility of a soil to liquefaction varies with the depth to groundwater. Natural hydrologic processes and human activities can cause groundwater levels to fluctuate over time. Therefore, it is impossible to predict depths to saturated soils during future earthquakes. One method of addressing time-variable depth to saturated soils is to establish a high groundwater level based on historical groundwater data. In areas where groundwater is either currently near surface or could return to near-surface levels within a land-use planning interval of 50 years, CGS constructs regional contour maps that depict highest historical depths to groundwater surface. Plate 1.3 depicts groundwater basins and contours reflecting the present or historic-high depth to groundwater surface within the project area.

Groundwater Basins

The study area lies within the San Francisco Bay hydrologic region and covers the California Department of Water Resources (CDWR, 2022) designated Santa Clara Valley Groundwater

Basin (number 2-9), which includes four subbasins, one of which, the East Bay Plain Subbasin, covers most of the study area. The basin is bounded by the Berkeley Hills on the northeast and San Francisco Bay on the southwest. Elevations within the basin in the project area range from 0 meters (0 feet) down by the San Francisco Bay up to 43 meters (140 feet) at the mouth of Wildcat Canyon, and up to 68 meters (225 feet) at the highest alluvial deposits along San Pablo Creek drainage below the San Pablo Dam. The Wildcat Creek and San Pablo Creek collect water from the Berkeley and Richmond hills in the northeast corner of the Richmond Quadrangle. They drain the hills and flow westward into the San Pablo Bay. Cerrito Creek runs along the boundary with Alameda County in the south. Several creeks flow northwestwards to the northeast of the East Bay Groundwater Subbasin watershed boundary, such as Refugio Creek, Garrity Creek, and Pinole Creek. Water bearing formations are mainly Quaternary alluvial deposits (**Qhty**, **Qhc**, **Qha**, **Qhf**, **Qht**, **Qpf, Qof, Qhf, Qhff, Qhfy, Qhl**, **Qoa, Qbt**). Aquifer storage coefficients typically indicate unconfined conditions at depths less than 100 feet. Natural recharge occurs by infiltration of water from streams emanating from the upland areas and direct rainfall percolation. Mean annual precipitation in the study area (30-year normal) ranges from 20 to 24 inches (https://prism.oregonstate.edu/normals/). The region has a Mediterranean climate with most of the precipitation in the region occurring as rain during the late fall, winter, and early spring.

Groundwater Data

For this study, groundwater conditions were investigated in the alluvial valleys within the project area. The evaluation was based on first-encountered, unconfined water noted in geotechnical borehole logs acquired from the planning departments at Contra Costa County and the cities of Richmond, Pinole, San Pablo, and Hercules, and the State Water Resources Control Board on GeoTracker (CWRCB, 2022) These datasets reflect water levels from 1930 to 2020. As they represent a measurement at a point in time, this information is only valuable when compared to measurements in neighboring boreholes with an understanding of local seasonal variability. Only two voluntary monitoring wells that are part of the California Department of Water Resources Statewide Groundwater Elevation Monitoring (CDWR, 2022) are in the map area.

Water level data evaluated in this study include more than 25,000 groundwater measurements from over 1250 locations (Plate 1.3) collected from the 1930's through the 2020, with most records representing conditions of the past twenty years. Groundwater levels from all available records were spatially and temporally evaluated in a GIS database to constrain the estimate of historically shallowest groundwater for the project area. The historic-high groundwater map was modified, where warranted, with input from current ground surface water, such as active creeks, recharge ponds, detention basins, other water impoundments, and reservoirs. The depth to groundwater contours depicted on Plate 1.3 do not represent conditions at a particular point in time, as usually presented on typical groundwater contour maps, but rather the historic high groundwater levels anticipated for the project area.

Groundwater Levels

Historic-high groundwater depths are generally shallow (less than 10 feet below the ground surface) in the East Bay Plain and along the Wildcat, San Pablo, Garrity, Pinole, and Refugio Creek alluvial valleys, reflecting the presence of surface water in perennial creeks and water recharge conditions from upland areas. As the altitude increases at the water basin boundaries, the depth to measured groundwater typically increases.

Shallow water was also encountered and mapped in alluvial fans that spread out across the East Bay Plain, as well as along smaller unnamed valleys and canyons. These materials are seasonally saturated with increased precipitation, heavy runoff, and stream flow. The deepest depths to groundwater (greater than 20 feet below ground surface) can only be found at the thickest areas of alluvial fan deposits.

Geologic Material Testing

Liquefaction Hazard Zoning: In-Situ Penetration Resistance

Of value in liquefaction evaluations are logs that report the results of downhole standard penetration tests in alluvial materials. The Standard Penetration Test (SPT) provides a standardized measure of the penetration resistance of geologic deposits and is used as an index of soil density. For this reason, SPT results are a critical component of the Seed-Idriss Simplified Procedure, a method used by CGS and the geotechnical community to quantitatively analyze liquefaction potential of sandy and silty material. The SPT is an in-field test based on counting the number of blows required to drive a split-spoon sampler (1.375-inch inside diameter) one foot into the soil. The driving force is provided by dropping a 140-pound hammer weight 30 inches. The SPT method is formally defined and specified by the American Society for Testing and Materials in test method D1586 (ASTM, 2004). Recorded blow counts for non-SPT geotechnical sampling, where the sampler diameter, hammer weight or drop distance differs from that specified for an SPT (ASTM D1586), are converted to SPT-equivalent blow counts if reliable conversions can be made. The actual and converted SPT blow counts are normalized to a common-reference, effective-overburden pressure of 1 atmosphere (approximately 1 ton per square foot) and a hammer efficiency of 60 percent using a method described by Seed and Idriss (1982) and Seed and others (1985). This normalized blow count is referred to as $(N_1)_{60}$. Geotechnical borehole logs provided information on lithologic and engineering characteristics of Quaternary deposits within the study area.

For liquefaction hazard zoning in the project area, soils reports were collected from the planning departments at Contra Costa County and the cities of Richmond, San Pablo, Hercules, and Pinole. Additional borehole information was gathered from geotechnical evaluations at school sites reviewed by CGS under contract with the division of the State Architect (DSA). The data were entered into the CGS geotechnical GIS database. After an initial review process and data quality controls, 185 borehole logs were selected for this study.

Of the 185 geotechnical borehole logs analyzed in this study (Plate 1.1), most included blow-count data from SPTs or from penetration tests that allow reasonable blow count conversions to SPT-equivalent values. Few of the borehole logs collected, however, included all the information (e.g., soil density, moisture content, sieve analysis, etc.) required for an ideal analysis using the Seed-Idriss Simplified Procedure. For boreholes having acceptable penetration tests, liquefaction analysis is performed using either recorded density, moisture, and sieve test values or using averaged test values of similar materials.

Landslide Hazard Zoning: Laboratory Shear Strength

To evaluate the stability of geologic materials susceptible to landslide failure under earthquake conditions, the geologic map units were ranked and grouped based on their shear strength.

Shear strength data were compiled for each geologic map unit in the project area with additional data from adjoining areas and quadrangles (Richmond in Alameda County, Oakland East, Oakland West, Brentwood, Briones Valley, Las Trampas Ridge, see Appendix A). For geologic units where sufficient shear-strength laboratory data could not be acquired, field measurements of Geologic Strength Index (GSI) (Marinos and others, 2007) were collected and the Hoek-Brown Failure Criterion (Hoek and others, 2002) was used to estimate the overall geologic unit strength. The non-linear Hoek-Brown criterion is a rock mass characterization method which uses equations to relate rock mass classification through a Geological Strength Index (GSI) to the angle of internal friction of a rock mass. This method allows strength assessment based on collected data, mainly discontinuity density, discontinuity condition, and geologic material properties (Hoek and others, 2002; Marinos and others, 2007). A total of 16 shear tests were collected in the project area for bedrock units which were limited to two Tertiary geologic units (**Tgu, Tgl, Tgud**; **Tmu**). The locations of rock and soil samples taken for shear testing and GSI field measurements (Hoek-Brown) within the study area are shown on Plate 1.2. The Hoek-Brown tests were relied on heavily in this area as so few shear test measurements were documented.

Adverse bedding conditions were identified in only a few scattered areas, mostly within the Garrity Formation (**Tgu, Tgl, Tgud**), Briones Formation (**Tbr**), and Monterey Group (**Tsa, Tdi, Tmu, Tcgl**). These formations were divided on shear strength differences where possible between coarse-grained (higher strength) and fine-grained (lower strength) lithologies where possible. Shear strength values for the fine- and coarse-grained lithologies were applied respectively to areas of adverse and favorable bedding orientation as determined from structural and terrain data discussed above. The Garrity Formation has the greatest number of mapped landslides in the study area and resistant sandstone and conglomerate lithologies outcrop along the resistant ridge tops (e.g., northwest of Inspiration Point to Wildcat Peak and San Pablo Ridge to the northwest).

Geologic units were grouped based on similar angles of internal friction (average phi) and lithologic character from both measured phi and from Hoek-Brown phi estimates, where available. Mean phi values for each geologic map unit from shear tests, most of which were from neighboring quadrangles, and Hoek Brown GSI field measurements, and corresponding strength groups are summarized in Table 1.2. Group phi values were assigned for each strength group using the combined mean group phi data and scientific judgement, to create significantly distinct strength groups for the analysis. For each geologic strength group (Table 1.3) in the map area, the shear strength value was assigned and used in our slope stability analysis. A geologic material strength map was made based on the groupings presented in Table 1.3, and this map provides a spatial representation of material strength for use in the slope stability analysis.

As discussed in section 4, the criteria for landslide zone mapping state that all existing landslides mapped as definite, or probable are automatically included in the Seismic Hazard Zone for earthquake-induced landslides. Therefore, an evaluation of shear strength parameters for existing landslides is not necessary for the preparation of the zone map. However, in the interest of completeness for the material strength map, to provide relevant material strength information to project plan reviewers, and to allow for future revisions of our zone mapping procedures, we collect, and compile shear strength data considered representative of existing landslides within the quadrangle if available. The strength characteristics of existing landslides must be based on tests of the materials along the landslide slip surface. Ideally, shear tests of slip surfaces formed in each mapped geologic unit would be used. However, this amount of information is rarely available. We collect and compile primarily "residual" strength parameters from laboratory tests of slip surface materials tested in direct shear or ring shear test equipment. For the project area, strength parameters applicable to existing landslide planes were not available and are not included in this analysis.

Table 1.2. Summary of the shear strength statistics for the Richmond, Mare Island, and San Quentin quadrangles.

	Formation Name	Number of Tests	Mean/Median Phi (deg)	Mean Group Phi (deg)	No Data: Similar Lithology	Phi Values Used in Stability Analysis
GROUP 1	Tmb (fbc) Tdi	12 1	42/- (fbc) 38/-	42		40
GROUP 2	KJk Jsv Tcs Kfn Tbr Tg (sst/cgl) KJfm (fbc) Tn Ts Tro To Tub KJfy	11 28 7 13 17 8 11 3 1 1 3 1 2	32/32 31/33 32/30 32/- 31/- 35/-† 35/35 32/35 34/- 34/- 35/35 35/- 33	32	Fc Kfa KJfc Tbh Tbl Tbu Tms Tc	32
GROUP 3	Tcc af Qhc Qhf Qha Tsa Th Tcs KJfm	7 40 6 32 13 4 4 2 1	31/- 28/28 27/27 27 /26 32/30 29/27 29/27 25/- 27/-	28	ac, acf alf, adf fg Tt Tshc Qf Th Tsa	28

	Formation Name	Number of Tests	Mean/Median Phi (deg)	Mean Group Phi (deg)	No Data: Similar Lithology	Phi Values Used in Stability Analysis
GROUP 4	sp Tmb (abc) Qof Qpf Qhl KJfm (abc) Qhff Tglt	4 4 11 42 2 20 3 2	24/25 24/23 (abc) 24/23 24/24 23/23 21/23 (abc) 23/24 22/-	23	Qpa Qht Tcglt Tcgl Spm	23
GROUP 5	Qbt Qmt Tr Tg (shale, slt) Qbt	3 3 12 4 3	21/21 21/21 21/21 20/20 24/20	21	afem Tr Qhbm	20
GROUP 6	Qls Tmu	11 10	12/10 16/15	13		15

Table 1.3. Summary of shear strength groups for the Richmond, Mare Island, and San Quentin quadrangles, Contra Costa County.

GROUP 1	GROUP 2	GROUP 3	GROUP 4	GROUP 5	GROUP 6
Tmb (fbc) Tdi	Jsv KJk KJfy KJfm (fbc) Kfn Tcs Tbr Tn Ts Tro To Tub Tbh Tg (l,u,ud) (sst/cgl)	fg Tsa Tshc Th Tcc Tt Qf Qhc Qhf Qha af ac, acf alf, adf	KJfm (abc) sp spm Tcglt Tcgl Tmb (abc) Qof Qpf Qpa Qhl Qhff Qhl Qht	Tr Tg (l,u,ud) (shale) afem Qbt Qhbm Qmt	Qls Tmu

abc = adverse bedding condition; fbc = favorable bedding condition; Tg (l, u and ud) are lower, upper and undifferentiated Garrity Formation.

REFERENCES

American Society for Testing and Materials, 2004, Standard test method for penetration test and split-barrel sampling of soils, Test Method D1586-99, in Annual Book of ASTM Standards, v. 4.08.

Bishop, C.C., Knox, R.D., Chapman, R.H., Rodgers, D.A., and Chase, G.B., 1973, Geological and Geophysical Investigations for Tri-Cities Seismic Safety and Environmental Resources Study: California Division of Mines and Geology Preliminary Report 19, 444 p., 10 pl.

Brabb, E.E., 1983, Map showing direction and amount of bedding dip of sedimentary rocks in San Mateo County, California, U.S. Geological Survey Miscellaneous Investigations Map I1257C, scale 1: 62,500.

Burrough, P.A. and McDonnell, R.A., 1998, Principles of Geographic Information Systems, New York, Oxford University Press, 190p.

California Department of Water Resources (CDWR), 2003, California's Groundwater, Bulletin 118, http://www.groundwater.water.ca.gov/bulletin118/update2003

California Department of Water Resources (CDWR), 2022, California Statewide Groundwater Elevation Monitoring (CASGEM) Program, http://www.water.ca.gov/groundwater/casgem/

California Water Resources Control Board (CWRCB), 2022, California Protection Agency, GeoTracker Groundwater Ambient Monitoring & Assessment (GAMA) database, http://geotracker.waterboards.ca.gov/gama

Hoek. E., Caranza-Torres, C.T., and Corkum, B., 2002, Hoek–Brown failure criterion—2002 edition *in* Bawden, H.R., Bawden, W., Curran, J., and Telesnicki, M., *editors*, Proceedings of the Fifth North American Rock Mechanics Symposium (NARMS-TAC), University of Toronto Press, Toronto, pp 267–273.

Horn, B.K.P., 1981, Hill shading and the reflectance map: Proceedings of the IEEE, v. 69, no. 1, p.14-47.f

Knudsen, K.L., Sowers, J.M., Witter, R.C., Wentworth, C.M., and Helley, E.J., 2000, Description of mapping of quaternary deposits and liquefaction susceptibility, nine-county San Francisco Bay region, California: U.S. Geological Survey Open-File Report 00-444.

Marinos, P., Marinos, V., and Hoek, E., 2007, Geological Strength Index (GSI). A characterization tool for assessing engineering properties for rock masses *in* Olalla, C., Perucho, A., and Romana, M., *editors*, proceedings of the ISRM workshop W1: Madrid, Spain 2007: Taylor & Francis, p.13-21.

Seed, H.B., and Idriss, I.M., 1982, Ground motions and soil liquefaction during earthquakes: Monograph Series, Earthquake Engineering Research Institute, Berkeley, California, 134 p.

Seed, H.B., Tokimatsu, K., Harder, L.F., and Chung, R.M., 1985, Influence of SPT procedures in soil liquefaction resistance evaluations: Journal of Geotechnical Engineering, ASCE, v. 111, no. 12, p. 1,425-1,445.

Witter, R.C., Knudsen, K.L, Sowers, J.M., Wentworth, C.M., Koehler, R.D., Randolph, C.E., Brooks, S.K., and Gans, K.D., 2006, Maps of Quaternary deposits and liquefaction susceptibility in the central San Francisco Bay region, California: U.S. Geological Survey Open-File Report 2006-1037, http://pubs.usgs.gov/of/2006/1037/.

Imagery

Lidar Hillshade derived from the 1.5 m Lidar Digital Terrain Model (2010), source of illumination: 45° sun angle, and 90° and 315° sun azimuths.

Lidar Hillshade derived from the 1 m Lidar Digital Terrain Model (2018), source of illumination: 45° sun angle, and 90° and 315° sun azimuths.

APPENDIX A: SOURCES OF ROCK STRENGTH DATA

SOURCE	NUMBER OF LAB TESTS SELECTED	NUMBER OF HOEK-BROWN TESTS SELECTED
Richmond, Mare Island, and San Quentin Quadrangles, Contra Costa County	16	68
Richmond Quadrangle, Alameda County	225	-
Hayward Quadrangle	39	-
Newark Quadrangle	7	-
Palo Alto Quadrangle	6	-
Dublin Quadrangle	3	-
Oakland East Quadrangle	3	-
Total Number of Shear Tests	299	68

SECTION 2: GROUND MOTION ASSESSMENT

for the

RICHMOND, MARE ISLAND, AND SAN QUENTIN 7.5-MINUTE QUADRANGLES, CONTRA COSTA COUNTY, CALIFORNIA

using the

2018 NATIONAL SEISMIC HAZARD MODEL

by

Rui Chen
P.G. 8598

DEPARTMENT OF CONSERVATION
CALIFORNIA GEOLOGICAL SURVEY

Purpose of this Section

This section of the Seismic Hazard Zone Report presents an assessment of earthquake shaking hazards in the Richmond, Mare Island, and San Quentin quadrangles (project area). It includes an explanation of the probabilistic seismic hazard analysis model from which ground motion parameters are derived, and how these parameters are used to delineate liquefaction and earthquake-induced landslide hazard zones.

PROBABILISTIC SEISMIC HAZARD ANALYSIS MODEL

Probabilistic ground motions are calculated using the United States Geological Survey (USGS) probabilistic seismic hazard analysis (PSHA) model for the 2018 Update of the National Seismic Hazard Maps (NSHMs) (Petersen and others, 2020). This model replaces ground-motion models of Petersen and others (2015, 2014, and 2008), Frankel and others (2002), Cao and others (2003) and Petersen and others (1996) used in previous official Seismic Hazard Zone maps. Like previous models, the 2018 USGS PSHA model utilizes the best available science, models, and data; and is the product of an extensive effort to obtain consensus within the scientific and engineering communities regarding earthquake sources and ground motions. In California, two earthquake source models control ground motion hazards, namely version three of the Uniform California Earthquake Rupture Forecast model (Field and others, 2013; 2014) and the Cascadia Subduction Zone model (Frankel and others, 2014). For shallow crustal earthquakes, ground motions are calculated using the Next Generation Attenuation Relations for Western U.S. (NGA-West2) developed from a Pacific Earthquake Engineering Research Center ground motion research project (Bozorgnia and others, 2014). The NGA-West2 used in the 2018 update of the NSHMs includes four ground motion models (GMMs): Abrahamson and others (2014), Boore and others (2014), Campbell and Bozorgnia (2014), and Chiou and Youngs (2014). For subduction zone earthquakes and earthquakes of other deep sources, GMMs developed specifically for such sources are used, including the Zhao and others (2006), Atkinson and Macias (2009), and BC Hydro (Addo and others, 2012).

In PSHA, ground motion hazards from potential earthquakes of all magnitudes and distances on all potential seismic sources are integrated. GMMs are used to calculate the shaking level from each earthquake based on earthquake magnitude, rupture distance, type of fault rupture (strike-slip, reverse, normal, or subduction), and other parameters such as time-average shear-wave velocity in the upper 30 meters beneath a site (V_{S30}). In CGS seismic hazards mapping applications prior to 2017, a uniform firm-rock site condition was assumed in PSHA calculation, and, in a separate post-PSHA step, National Earthquake Hazard Reduction Program amplification factors were applied to adjust all sites to a uniform alluvial soil condition to approximately account for the effect of site condition on ground motion amplitude. In the current application, site effect is directly incorporated in PSHA via GMM scaling. Specifically, V_{S30} is built into GMMs as one of the predictor variables and, therefore, it is an input parameter in the PSHA calculation. The V_{S30} value at each grid point is assigned from a geology- and topography-based V_{S30} map for California developed by Wills and others (2015). The statewide V_{S30} map consists of fifteen V_{S30} groups with group mean V_{S30} values ranging from 176 m/s to 733 m/s. It is to be noted that these values are not determined from site-specific velocity data. Some group values have considerable uncertainties as indicated by a coefficient of variation ranging from 11% in Quaternary (Pleistocene) sand deposits to 55% in crystalline rocks.

For landslide zoning purposes, ground motions are calculated at each grid point of a 0.005-degree grid (approximately 500-meter spacing) that adequately covers the entire quadrangle. A V_{S30} map and grid points in the project area are depicted in Plate 2.1. For liquefaction zoning purposes, ground motions are calculated at each boring location. For site investigation, it is strongly recommended that V_{S30} be determined from site-specific shear wave velocity profile data.

PSHA provides more comprehensive characterizations of ground motion hazards compared to traditional scenario-based analysis by integrating hazards from all earthquakes above a certain magnitude threshold. However, many applications of seismic hazard analyses, including CGS' liquefaction and earthquake-induced landslide hazard mapping analyses, still rely on scenario earthquakes or some aspects of scenario earthquakes. Deaggregation enables identification of the most significant scenario or scenarios in terms of magnitude and distance pair. Deaggregation is often performed for a particular site, a chosen ground motion parameter (such as peak ground acceleration or PGA), and a predefined exceedance probability level (i.e., hazard level). As in previous regulatory zone maps, the ground motion hazard level for liquefaction and earthquake-induced landslide hazard zoning is 10% exceedance probability in 50 years or 475-year return period.

Probabilistic ground motion calculation and hazard deaggregation are performed using USGS hazard codebase, nshmp-haz version 1.3.0, a Java library developed in support of the USGS NSHM project. The Java code library is hosted in GitHub and is publicly available at: https://github.com/usgs/nshmp-haz/. This codebase also supports the USGS web-based site-specific ground motions calculator, the Unified Hazard Tool, https://earthquake.usgs.gov/hazards/interactive/. The source model used for the published 2018 NSHMs is adopted in its entirety. The 2018 source model is also hosted in GitHub and is publicly available at: https://github.com/usgs/nshm-cous-2018.

APPLICATION TO LIQUEFACTION AND EARTHQUAKE-INDUCED LANDSLIDE HAZARD ASSESSMENT

The current CGS liquefaction hazard analysis approach requires that PGA be scaled by an earthquake magnitude weighting factor (MWF) to incorporate a magnitude-correlated duration effect (California Geological Survey, 2004; 2008). The MWF-scaled PGA is referred to as pseudo-PGA and is used as Liquefaction Opportunity (see Section 3 of this report). The MWF calculation is straight forward for a scenario earthquake. In PSHA, however, earthquakes of different magnitudes and distances contribute differently to the total hazard at a chosen probabilistic PGA level. The CGS approach to MWF calculation is based on binned magnitude-distance deaggregation. At each location, an MWF is calculated for each magnitude-distance bin and is weighted by the contribution of that magnitude-distance bin to the total hazard. The total MWF is the sum of probabilistic hazard-weighted MWFs from all magnitude-distance bins. This approach provides an improved estimate of liquefaction hazard in a probabilistic sense. All magnitudes contributing to the hazard estimate are used to weight the probabilistic calculation of PGA, effectively causing the cyclic stress ratio liquefaction threshold curves to be scaled probabilistically when computing factor of safety. This procedure ensures that large, distant earthquakes that occur less frequently but contribute *more,* and smaller, more frequent events that contribute *less* to the liquefaction hazard are appropriately accounted for (Real and others, 2000).

The current CGS earthquake-induced landslide hazard analysis approach requires the probabilistic PGA and a predominant earthquake magnitude to estimate cumulative Newmark displacement for a given rock strength and slope gradient condition using a regression equation, described more fully in Section 4 of this report. The predominant earthquake magnitude is chosen to be the modal magnitude from deaggregation.

Pseudo-PGA and probabilistic PGA at grid points are depicted in Plates 2.2 and 2.3. Modal magnitude is depicted in Plate 2.4. Ground motion generally increases based on the distance from the Hayward fault trace that cuts northwestward across the quadrangles from the southeast corner. Shaking hazards are controlled predominantly by the Hayward fault, with increasing contribution from the San Andreas fault towards the southwest of the map area. Other sources that contribute to shaking hazards include Calaveras and Rodger's Creek faults, and background (gridded) seismicity. Modal magnitudes (Plate 2.4) reflect the magnitudes of earthquakes that the Hayward fault can produce for most of the area but increases to the southwest as influence from the San Andreas fault system exceeds that of the Hayward fault. Ground motion distribution is controlled by proximity to the faults and is affected by subsurface geology. Topographic effects on ground motion are not considered in our analysis at this time. In general, when fault distances are similar, expected PGA is higher where there are softer Quaternary sediments (lower V_{S30} values) and lower where there are harder volcanic and crystalline rocks (higher V_{S30} values). The table below summarizes ranges of PGA, pseudo-PGA, modal magnitude, and V_{S30} values expected in the quadrangle.

Table 2.1. Summary of ground motion parameters used for liquefaction and earthquake-induced landslide analyses.

PGA (g)	Pseudo-PGA (g)	Modal Magnitude	V_{S30} (m/s)
0.44 – 0.67	0.36 – 0.57	6.28 – 7.11	176 – 733

REFERENCES

Abrahamson, N.A., Silva, W.J., and Kamai, R., 2014, Summary of the ASK14 ground motion relation for active crustal regions: Earthquake Spectra, vol. 30, p. 1025–1055.

Addo, K., Abrahamson, N., and Youngs, R. (BC Hydro), 2012, Probabilistic seismic hazard analysis (PSHA) model—Ground motion characterization (GMC) model: Report E658, published by BC Hydro.

Atkinson, G.M., and Macias, M., 2009, Predicted ground motions for great interface earthquakes in the Cascadia subduction zone: Bulletin of the Seismological Society of America, vol. 99, p. 1,552–1,578.

Boore, D.M., Stewart, J.P., Seyhan, E., and Atkinson, G.M., 2014. NGA-West2 equations for predicting PGA, PGV, and 5% damped PSA for shallow crustal earthquakes: Earthquake Spectra, vol. 30, p. 1057–1085.

Bozorgnia Y., Abrahamson, N.A., Atik, L.A., Ancheta T.D., and others, 2014, NGA-West2 Research Project: Earthquake Spectra, vol 30, no. 3, p. 973 –987, DOI: 10.1193/072113EQS209M.

Campbell, K.W., and Bozorgnia, Y., 2014, NGA-West2 ground motion model for the average horizontal components of PGA, PGV, and 5% damped linear acceleration response spectra: Earthquake Spectra, vol. 30, p. 1087–1115.

California Geological Survey, 2008, Guidelines for evaluating and mitigating seismic hazards in California: California Geological Survey Special Publication 117a, 98 p. Available on-line at: http://www.conservation.ca.gov/cgs/publications/sp117a.

California Geological Survey, 2004, Recommended criteria for delineating seismic hazard zones in California: California Geological Survey Special Publication 118, 12 p. Available on-line at: http://www.conservation.ca.gov/cgs/publications/sp118.

Cao, T., Bryant, W.A., Rowshandel, B., Branum, D. and Wills, C.J., 2003, The Revised 2002 California Probabilistic Seismic Hazard Maps. California Geological Survey, Online Report: http://www.conservation.ca.gov/cgs/Documents/PSHA/2002%20California%20Hazard%20Maps.pdf.

Chiou, B.S.-J., and Youngs, R.R., 2014. Update of the Chiou and Youngs NGA model for the average horizontal component of peak ground motion and response spectra: Earthquake Spectra, vol. 30, p. 1117–1153.

Field, E.H., Biasi, G.P., Bird, P., Dawson, T.E., Felzer, K.R., Jackson, D.D., Johnson, K.M., Jordan, T.H., Madden, C., Michael, A.J., Milner, K.R., Page, M.T., Parsons, T., Powers, P.M., Shaw, B.E., Thatcher,W.R., Weldon, II, R.J., and Zeng, Y., 2013, Uniform California Earthquake Rupture Forecast, Version 3 (UCERF3)—The Time-Independent Model, U.S. Geological Survey Open-File Report 2013–1165, California Geological Survey Special Report 228, and Southern California Earthquake Center Publication 1792, 97 pp., available at http://pubs.usgs.gov/of/2013/1165/.

Field, E.H., Arrowsmith, R.J., Biasi, G.P., Bird, P., Dawson, T.E., Felzer, K.R., Jackson, D.D., Johnson, K.M., Jordan, T.H., Madden, C., Michael, A.J., Milner, K.R., Page, M.T., Parsons, T., Powers, P.M., Shaw, B.E., Thatcher, W.R., Weldon, II, R.J., and Zeng, Y., 2014, Uniform California earthquake rupture forecast, Version 3 (UCERF3) —The time independent model: Bulletin of Seismological Society of America, vol. 104, p. 1122–1180.

Frankel, A.D., Petersen, M.D., Muller, C.S., Haller, K.M., Wheeler, R.L., Layendecker, E.V., Wesson, R.L., Harmsen, S.C., Cramer, C.H., Perkins, D.M., and Rukstales, K.S., 2002, Documentation for the 2002 Update of the National Seismic Hazard Maps: U.S. Geological Survey, Open-File Report 02-420, 33 p.

Frankel, A., Chen, R., Petersen, M., Moschetti, M., and Sherrod, B., 2014, 2014 Update of the Pacific Northwest Portion of the U.S. National Seismic Hazard Maps: Earthquake Spectra, vol. 31, no. S1, p. S131–S148, DOI: 10.1193/111314EQS193M.

Petersen, M.D., Bryant, W.A., Cramer, C.H., Cao, T., Reichle, M.S., Frankel, A.D., Lienkaemper, J.J., McCrory, P.A. and Schwartz, D.P., 1996, Probabilistic seismic hazard assessment for the State of California: California Department of Conservation, Division of Mines and Geology Open-File Report 96-08; also U.S. Geological Survey Open-File Report 96-706, 33 p.

Petersen, M.D., Frankel, A.D., Harmsen, S.C., Mueller, C.S., Haller, K.M., Wheeler, R.L., Wesson, R.L., Zeng, Y., Boyd, O.S., Perkins, D.M., Luco, N., Field, E.H., Wills, C.J., and Rukstales, K.S., 2008, Documentation for the 2008 update of the United States National Seismic Hazard Maps: U.S. Geol. Survey Open-File Report 2008-1XXX, 60p.

Petersen, M.D., Moschetti, M.P., Powers, P.M., Mueller, C.S., Haller, K.M., Frankel, A.D., Zeng, Y., Rezaeian, S., Harmsen, S.C., Boyd, O.S., Field, N., Chen, R., Rukstales, K.S., Luco, N., Wheeler, R.L., Williams, R.A., and Olsen, A.H., 2014, Documentation for the 2014 update of the United States national seismic hazard maps, U.S. Geol. Survey. Open-File Rept. 2014-1091, 243 pp., doi: 10.3133/ofr20141091.

Petersen, M.D., Moschetti, M.P., Powers, P.M., Mueller, C.S., Haller, K.M., Frankel, A.D., Zeng, Y., Rezaeian, S., Harmsen, S.C., Boyd, O.S., Field, N., Chen, R., Rukstales, K.S., Luco, N., Wheeler, R.L., Williams, R.A., and Olsen, A.H., 2015, The 2014 United States national seismic hazard model: Earthquake Spectra, vol. 31, no. S1, p. S1–S30, doi: 10.1193/120814EQS210M.

Petersen, M.D., Shumway, A.M., Powers, P.M., Mueller, C.S., Haller, K.M., Moschetti, M.P, Frankel, A.D., Rezaeian, S., McNamara, D.E., Luco, N., Boyd, O.S., Rukstales, K.S., Jaiswal, K.S., Thompson, E.M., Hoover, S.M., Clayton, B.S., Field, E.H., and Zeng, Y., 2020, The 2018 updated of the US National Seismic Hazard Model: Overview of model and implications: Earthquake Spectra, vol. 36, no. 1, p. 5–41, doi: 10.1177/8755293019878199.

Real, C.R., Petersen, M.D., McCrink, T.P. and Cramer, C.H., 2000, Seismic Hazard Deaggregation in zoning earthquake-induced ground failures in southern California: Proceedings of the Sixth International Conference on Seismic Zonation, November 12-15, Palm Springs, California, EERI, Oakland, CA.

Wills, C.J., Gutierrez, C.I., Perez, F.G., and Branum, D.M., 2015, A next-generation V_{S30} map for California based on geology and topography: Bulletin of Seismological Society of America, vol. 105, no. 6, p. 3083–3091, doi: 10.1785/0120150105.

Zhao, J.X., Zhang, J., Asano, A., Ohno, Y., Oouchi, T., Takahashi, T., Ogawa, H., Irikura, K., Thio, H.K., Somerville, P.G., Fukushima, Y.A, and Fukushima, Y., 2006, Attenuation relations of strong ground motion in Japan using site classification based on predominant period: Bulletin of the Seismological Society of America, v. 96, p. 898–913.

SECTION 3: EVALUATION OF LIQUEFACTION HAZARD

in the

RICHMOND, MARE ISLAND, AND SAN QUENTIN 7.5-MINUTE QUADRANGLES, CONTRA COSTA COUNTY, CALIFORNIA

by

Jacqueline Bott
P.G. 7459 C.E.G. 2382

Department of Conservation
California Geological Survey

Purpose of this Section

This Section of the Seismic Hazard Zone Report summarizes the analyses and criteria used to delineate liquefaction hazard zones in the Richmond, Mare Island, and San Quentin quadrangles (project area).

ZONING TECHNIQUES

Liquefaction may occur in water-saturated sediment during moderate to great earthquakes. When this occurs, sediment loses strength and may fail, causing damage to buildings, bridges, and other structures. Many methods for mapping liquefaction hazard have been proposed. Youd (1991) highlights the principal developments and notes some of the widely used criteria. Youd and Perkins (1978) demonstrate the use of geologic criteria as a qualitative characterization of liquefaction susceptibility and introduce the mapping technique of combining a liquefaction susceptibility map and a liquefaction opportunity map to produce a liquefaction potential map. Liquefaction susceptibility is a function of the capacity of sediment to resist liquefaction, whereas liquefaction opportunity is a function of potential seismic ground shaking intensity.

The method applied in this study to evaluate liquefaction potential is similar to that Tinsley and others (1985) used to map liquefaction hazards in the Los Angeles region. These investigators, in turn, applied a combination of the techniques developed by Seed and others (1983) and Youd and Perkins (1978). CGS's method combines geologic mapping, geotechnical assessment of soils, hydrogeological and historical groundwater analyses, and probabilistic earthquake ground motions employing criteria adopted by the State Mining and Geology Board (CGS, 2004).

Liquefaction Susceptibility

Liquefaction susceptibility reflects the relative resistance of a soil to loss of strength when subjected to ground shaking. Physical properties of soil such as sediment grain-size distribution, compaction, cementation, saturation, and depth from the surface govern the degree of resistance to liquefaction. Some of these properties can be correlated to a deposit's geologic age and environment of deposition. With increasing age, relative density may increase through cementation of the particles or compaction caused by the weight of the overlying sediment.

Grain-size characteristics of a soil also influence susceptibility to liquefaction. Sand is more susceptible than silt or gravel, although silt of low plasticity is treated as liquefiable in this investigation. Cohesive soils generally are not considered susceptible to liquefaction. Such soils may be vulnerable to strength loss with remolding and represent a hazard that is not specifically addressed in this investigation. Soil characteristics that result in higher measured penetration resistances generally indicate lower liquefaction susceptibility. In summary, soils that lack resistance (susceptible soils) typically are saturated, loose, and granular. Soils resistant to liquefaction include all soil types that are dry, cohesive, or sufficiently dense.

CGS's inventory of areas containing soils susceptible to liquefaction begins with evaluation of historical occurrences of liquefaction, geologic maps, cross-sections, geotechnical test data, geomorphology, and groundwater hydrology. Soil properties and soil conditions such as type, age, texture, color, and consistency, along with historic-high depths to groundwater are used to identify, characterize, and correlate susceptible soils. Because Quaternary geologic mapping is based on observable similarities between soil units, liquefaction susceptibility maps typically are often similar to Quaternary geologic maps, depending on local groundwater levels. CGS's qualitative relations among susceptibility, geologic map unit, and depth to ground water are summarized in Table 3.1.

In the past, gravelly soils were considered not to be susceptible to liquefaction because the high permeability of these soils presumably would allow the dissipation of pore pressures before liquefaction could occur. However, liquefaction in gravelly soils has been observed during earthquakes, and recent laboratory studies have shown that gravelly soils are susceptible to liquefaction (Ishihara, 1985; Harder and Seed, 1986; Budiman and Mohammadi, 1995; Evans and Zhou, 1995; and Sy and others, 1995). SPT-derived density measurements in gravelly soils are unreliable and generally too high. They are likely to lead to overestimation of the density of the soil and, therefore, result in an underestimation of the liquefaction susceptibility. To identify potentially liquefiable units where the N values appear to have been affected by gravel content, correlations were made with boreholes in the same unit where the N values do not appear to have been affected by gravel content.

Table 3.1. Liquefaction susceptibility of Quaternary units in the Richmond, Mare Island, and San Quentin quadrangles.

Geologic Map Unit	Age	Sediment/Material Type	Consistency	Liquefaction Susceptibility*
ac, af, adf, alf, acf	Historical	Sand, silt, gravel, clay, cobbles, concrete	Loose to dense	Variable
afem	Historical	Sand, silt, gravel, clay, cobbles, concrete	Loose	Very High
Qhc, Qhly	Latest Holocene to Holocene	Sand, gravel, cobbles, silt, clay	Loose	Very High
Qhfy, Qhty	Latest Holocene to Holocene	Sand, gravel, silt, clay	Loose to dense	High
Qhl	Holocene	Sand, silt, clay	Loose	High
Qha, Qht	Holocene	Gravel, sand, silt, clay	Loose to dense	High
Qhf,	Holocene	Gravel, sand, silt, clay	Loose to dense	High
Qhff, Qhbm	Holocene	Silt, clay	Loose to dense	Moderate
Qa, Qf	Holocene to Latest Pleistocene	Gravel, sand, silt, clay	Loose to dense	Moderate
Qpf, Qpa	Latest Pleistocene	Gravel, sand, silt, clay	Moderately dense to dense	Low
Qmt, Qbt	Pleistocene	Sand, Silt, clay	Moderately dense to dense	Low
Qoa, Qof, Qop,	Pleistocene	Sand, gravel, silt, clay	Dense to very dense	Very Low

*When saturated

Ground Motion for Liquefaction Opportunity

Ground motion calculations used by CGS for regional liquefaction zonation assessments are based on the probabilistic seismic hazard analysis (PSHA) model developed by the United States Geological Survey (USGS) (Petersen and others, 2020) for the 2018 Update of the United States National Seismic Hazard Maps. The model calculates ground motion in terms of peak horizontal ground acceleration (PGA) at a 10 percent in 50 years exceedance probability level. For liquefaction analysis, CGS modifies probabilistic PGA by a scaling factor that is a function of magnitude. Calculation of the scaling factor is based on binned magnitude-distance deaggregation of seismic source contribution to total shaking. The result is a magnitude-weighted, pseudo-PGA that CGS refers to as Liquefaction Opportunity (LOP). This approach provides an improved estimate of liquefaction hazard in a probabilistic sense, ensuring that the effects of large, infrequent, distant earthquakes, as well as smaller, more frequent, nearby events are appropriately accounted for (Real and others, 2000). These weighted, pseudo-PGA ground motion values are used to calculate the seismic load imposed on a soil column, expressed as the cyclic stress ratio (CSR). A more detailed description of the development of ground shaking opportunity data and parameters used in liquefaction hazard zoning can be found in Section 2 of this report.

Liquefaction Analysis

CGS performs a quantitative analysis of geotechnical data to evaluate liquefaction potential using an in-house developed computer program based on the Seed-Idris Simplified Procedure (Seed and Idriss, 1971; Seed and others, 1983; National Research Council, 1985; Seed and others, 1985; Seed and Harder, 1990; Youd and Idriss, 1997; Youd and others, 2001). The calculations and correction factors used in the program are taken directly from the equations in Youd and others (2001).

The program calculates the liquefaction potential of each non-clay soil layer encountered at a test-drilling site that includes at least one SPT. CGS defines soil layers with a factor of safety (FS) relative to liquefaction hazard of 1.0 or less as potentially liquefiable. The FS is defined as the ratio of cyclic resistance ratio (CRR), which reflects the resistance to liquefaction of the soil layer, to cyclic stress ratio (CSR), which represents the seismic load on the layer. Input parameters for calculation of CRR include SPT results, groundwater level, soil density, grain-size analysis, moisture content, soil type, and sample depth. The CSR is calculated using the pseudo-PGA provided in the ground motion analysis.

The FS is calculated for each layer in the soil column at a given borehole. The minimum FS value of all the layers penetrated by the borehole determines the liquefaction potential for that borehole location. CGS geologists use the results of this analysis, the groundwater analysis, and geologic conditions to determine the final liquefaction hazard zone.

Liquefaction Zoning Criteria

Areas underlain by materials susceptible to liquefaction during an earthquake are included in liquefaction zones using criteria developed by the Seismic Hazards Mapping Act Advisory Committee and adopted by the SMGB (CGS, 2004). Under those guideline criteria, liquefaction zones are areas meeting one or more of the following:

1) Areas known to have experienced liquefaction during historical earthquakes.
2) All areas of uncompacted artificial fill that are saturated, nearly saturated, or may be expected to become saturated.
3) Areas where sufficient existing geotechnical data and analyses indicate that the soils are potentially liquefiable.
4) Areas where existing subsurface data are not sufficient for quantitative evaluation of liquefaction hazard. Within such areas, zones may be delineated by geologic criteria as follows:
    a) Areas containing soil deposits of late Holocene age (current river channels and their historic floodplains, marshes, and estuaries), where the M7.5-weighted peak acceleration that has a 10 percent probability of being exceeded in 50 years is greater than or equal to 0.10 g and the anticipated depth to saturated soil is less than 40 feet; or
    b) Areas containing soil deposits of Holocene age (less than 11,700 years), where the M7.5-weighted peak acceleration that has a 10 percent probability of being exceeded in 50

years is greater than or equal to 0.20 g and the anticipated depth to saturated soil is less than 30 feet; or

c) Areas containing soil deposits of latest Pleistocene age (11,700 to 15,000 years), where the M7.5-weighted peak acceleration that has a 10 percent probability of being exceeded in 50 years is greater than or equal to 0.30 g and the anticipated depth to saturated soil is less than 20 feet.

Application of the above criteria allows compilation of Earthquake Zones of Required Investigation for liquefaction hazard, which are useful for preliminary evaluations, general land-use planning and delineation of special studies zones (Youd, 1991).

Delineation of Liquefaction Hazard Zones

Upon completion of a liquefaction hazard evaluation within a project quadrangle, CGS applies the above criteria to its findings to delineate Seismic Hazard Zones for liquefaction. Based on the evaluation, about 57.5 square kilometers (22.3 square miles) of the project area are included in the Seismic Hazard Zone for liquefaction. Following is a description of the criteria-based factors that governed the construction of the Seismic Hazard Zone Map for the project area.

Areas of Past Liquefaction

Only two documented observations of historical liquefaction are recorded for the area encompassed by the Richmond and Mare Island quadrangles (Tinsley and others, 1998, Youd and Hoose, 1978). Lateral spread, settlement, and sand boils were observed at the end of the Point Richmond Ferry Terminal during the 1989 Loma Prieta earthquake in artificial fill over San Francisco Bay mud. Settlement was observed for the 1906 San Francisco earthquake near the mouth of Garrity Creek again in an area of artificial fill emplaced over San Francisco Bay mud.

Artificial Fills

Artificial fills in the project area large enough to show at the scale of project mapping (1:24,000) cover approximately 12.6 square kilometers (4.9 square miles) in the project area, consisting of artificial fill over San Francisco Bay mud along the bay front. In addition, artificial engineered fill areas are mapped for river channels and levees, detention basins, elevated freeways, as well as isolated bodies of fill typically associated with construction projects of various sizes. Zoning for liquefaction in artificial fills depends on soil properties and groundwater conditions in underlying strata.

Areas with Sufficient Existing Geotechnical Data

Most of the borehole logs evaluated for liquefaction potential using the Seed-Idriss Simplified Procedure are located in developed areas in the alluvial fans surrounding Wildcat and San Pablo creeks in the East Bay Plain. Analysis of blow count values and other soil property measurements reported in the logs indicate that most of the boreholes situated in Holocene and Latest Pleistocene deposits penetrate saturated layers of loose sand, gravel, and silt that may liquefy under the expected earthquake loading. These deposits include modern stream channel deposits (**Qhc**), Holocene alluvial fan levee deposits (**Qhly**, **Qhl**), Holocene & Latest Pleistocene undifferentiated alluvial sediments (**Qha, Qa**), Holocene to Latest Pleistocene alluvial fan deposits (**Qhfy**, **Qhf, Qhff, Qf, Qpf**), and even Early to Late Pleistocene alluvial fan deposits (**Qof**) mapped along and adjacent to the downstream end of creeks. In addition, this includes areas mapped as artificial fill emplaced over San Francisco Bay mud (**afem**). Of note, areas mapped as **Qof** contain borings that indicate that Yerba Buena Mud, dated as 75 to 125 ka, is found at depths of 40 to 50 feet. These older alluvial deposits were found to contain liquefiable layers and are thus included in the Seismic Hazard Zone, despite their designated liquefaction susceptibility of very low based on Witter and others (2006).

Certain areas of the alluvial fan deposits from the San Pablo and Wildcat creeks have been extensively graded and the subsurface geology recorded in the boring logs consists of consolidated fill materials that are not liquefiable according to the Seed-Idriss Simplified Procedure.

Areas with Insufficient Existing Geotechnical Data

In areas with insufficient geotechnical data coverage, Quaternary sedimentary deposits were evaluated for seismic hazard zonation based on geologic factors, groundwater levels, and extrapolation of known soil conditions in adjacent areas. Adequate geotechnical borehole information is lacking for the Early to Late Pleistocene pediment mapped at the foot of the Berkeley Hills close to the border with Alameda County in the southern portion of the Richmond Quadrangle. There are also few geotechnical borings along alluvial valleys and smaller unnamed connected valleys and canyons. The Quaternary units mapped in these areas typically contain varying amounts of loose, granular materials that are saturated because of the presence of near-surface groundwater following rainfall events and proximity to streams and generally have shallow groundwater. Those conditions, along with the ground motions expected to occur in the region, combine to form a sufficient basis for including these areas in the Seismic Hazard Zone for liquefaction.

ACKNOWLEDGMENTS

The authors thank the following individuals and organizations for their assistance in obtaining the data necessary to complete this project: Chris Castanchoa and Yader Bermudez of the City of Richmond, Jamie Aldred of the City of Pinole, Darwin Myers of Contra Costa County, and Jeff Balantine from the City of El Cerrito for review comments . At CGS, Alexa Evans and Daniel Langermann assisted with geotechnical data collection and entry efforts. Bob Moskovitz and Jonathan Goergen provided database compilation and analysis support. Kate Thomas and Michael Falsetto prepared the final Seismic Hazard Zone Map and prepared the graphic displays for this report. Tim Dawson and Erik Frost provided technical review for this report.

REFERENCES

American Society for Testing and Materials, 2004, Standard test method for penetration test and split-barrel sampling of soils, Test Method D1586-99, in Annual Book of ASTM Standards, v. 4.08.

Budiman, J.S., and Mohammadi, J., 1995, Effect of large inclusions on liquefaction of sands, in Evans, M.D., and Fragaszy, R.J., editors, Static and Dynamic properties of Gravelly Soils: American Society of Civil Engineers Geotechnical Special Publication no. 56, p. 48-63.

California Geological Survey, 2004, Recommended criteria for delineating seismic hazard zones in California: California Geological Survey Special Publication 118, 12 p. Available on-line at: http://www.conservation.ca.gov/cgs/shzp/webdocs/documents/sp118_revised.pdf.

Evans, M.D., and Zhou, S., 1995, Liquefaction behaviour of sand-gravel composites: American Society of Civil Engineers, Journal of Geotechnical Engineering, v. 121, no. 3, p. 287-298.

Harder, L.F., and Seed, H.B., 1986, Determination of penetration resistance for coarse-grained soils using the Becker hammer drill: University of California at Berkeley, College of Engineering, Earthquake Engineering Research Center, report no. UCB/EERC-86/06, 126 p.

Ishihara, K., 1985, Stability of natural deposits during earthquakes, in Proceedings of the Eleventh International Conference on Soil Mechanics and Foundation Engineering, San Francisco, v. 1, p. 321-376.

National Research Council Special Publication, Committee on Earthquake Engineering, National Academy Press, Washington, D.C., 240 p.

Petersen, M.D., Shumway, A.M., Powers, P.M., Mueller, C.S., Haller, K.M., Moschetti, M.P, Frankel, A.D., Rezaeian, S., McNamara, D.E., Luco, N., Boyd, O.S., Rukstales, K.S., Jaiswal, K.S., Thompson, E.M., Hoover, S.M., Clayton, B.S., Field, E.H., and Zeng, Y., 2020, The 2018 updated of the US National Seismic Hazard Model: Overview of model and implications: Earthquake Spectra, vol. 36, no. 1, p. 5–41, doi: 10.1177/8755293019878199.

Plafker, G., and Galloway, J.P., eds., 1989, Lessons learned from the Loma Prieta, California, earthquake of October 17, 1989: U.S. Geological Survey Circular 1045, 48 p.

Quantum Spatial, Inc., 2019, Northern California 3DEP QL1 QL2 LiDAR Project Report, report submitted to USGS under contract # G16PC00016.

Real, C.R., Petersen, M.D., McCrink, T.P., and Cramer, C.H., 2000, Seismic Hazard Deaggregation in zoning earthquake-induced ground failures in southern California: Proceedings of the Sixth International Conference on Seismic Zonation, November 12-15, Palm Springs, California, EERI, Oakland, CA.

Seed, H.B., and Idriss, I.M., 1971, Simplified procedure for evaluating soil liquefaction potential: Journal of the Soil Mechanics and Foundations Division of ASCE, v. 97: SM9, p. 1,249-1,273.

Seed, H.B., and Idriss, I.M., 1982, Ground motions and soil liquefaction during earthquakes: Monograph Series, Earthquake Engineering Research Institute, Berkeley, California, 134 p. Seed, H.B., Idriss, I.M., and Arango, I., 1983, Evaluation of liquefaction potential using field performance data: Journal of Geotechnical Engineering, v. 109, no. 3, p. 458-482.

Seed, H.B., Idriss, I.M., and Arango, I., 1983, Evaluation of liquefaction potential using field performance data: Journal of Geotechnical Engineering, v. 109, no. 3, p. 458-482.

Seed, H.B., Tokimatsu, Kohji, Harder, L.F., and Chung, R.M., 1985, Influence of SPT procedures in soil liquefaction resistance evaluations: Journal of Geotechnical Engineering, ASCE, v. 111, no. 12, p. 1,425-1,445.

Seed, R.B., Dickenson, S.E., Riemer, M.F., Bray, J.D., Sitar, N., Mitchell, J.K., Idriss, I.M., Kayen, R.E., Kropp, A., Harder, L.F., Jr., and Power, M.S., 1990, Preliminary report on the principal geotechnical aspects of the October 17, 1989, Loma Prieta earthquake, Earthquake Engineering Research Center, Report No. UCB/EERC-90/05.

Seed, R.B., and Harder, L.F., 1990, SPT-based analysis of cyclic pore pressure generation and undrained residual strength: Proceedings of the H. Bolton Seed Memorial Symposium, v. 2, p. 351-376.

Sy, A., Campanella, R.G., and Stewart, R.A., 1995, BPT-SPT correlations for evaluations of liquefaction resistance in gravelly soils, in Evans, M.D., and Fragaszy, R.J., editors, Static and Dynamic Properties of Gravelly Soils: American Society of Civil Engineers Geotechnical Special Publication no. 56, p. 1-19.

Tinsley, J.C., Youd, T.L., Perkins, D.M., and Chen, A.T.F., 1985, Evaluating liquefaction potential, in Ziony, J.I., editor, Evaluating earthquake hazards in the Los Angeles region — An earth science perspective: U.S. Geological Survey Professional Paper 1360, p. 263-316.

Tinsley, J.C., III, Egan, J.A., Kayen, R.E., Bennett, M.J., Kropp, A., and Holzer, T.L., 1998, Appendix: Maps and descriptions of liquefaction and associated effects: in Holzer, T.L., ed., The Loma Prieta, California, Earthquake of October 17, 1989 - Liquefaction: U.S. Geological Survey Professional Paper 1551-B.

Youd, T.L., 1973, Liquefaction, flow and associated ground failure: U.S. Geological Survey Circular 688, 12 p.

Youd, T.L., and Perkins, D.M., 1978, Mapping liquefaction-induced ground failure potential: Journal of Geotechnical Engineering, v. 104, p. 433-446.

Youd, T.L., and Hoose, S.N., 1978, Historical ground failures in Northern California triggered by earthquakes: U.S. Geological Survey Professional Paper 993.

Youd, T.L., 1991, Mapping of earthquake-induced liquefaction for seismic zonation: Earthquake Engineering Research Institute, Proceedings, Fourth International Conference on Seismic Zonation, v. 1, p. 111-138.

Youd, T.L., and Idriss, I.M., 1997, editors, Proceedings of the NCEER workshop on evaluation of liquefaction resistance of soils: National Center for Earthquake Engineering Research Technical Report NCEER-97-0022, 276 p.

Youd, T.L., Idriss, I.M., Andrus, R.D., Arango, I., Castro, G., Christian, J.T., Dobry, R., Finn, W.D.L., Harder, L.F. Jr., Hynes, M.E., Ishihara, K., Koester, J.P., Liao, S.S.C., Marcusson, W.F., Martin, G.R., Mitchell, J.K., Moriwaki, Y., Power, M.S., Robertson, P.K., Seed, R.B., and Stokoe, K.H., 2001, Liquefaction resistance of soils; Summary report from the 1996 NCEER and 1998 NCEER/NSF workshops on evaluation of liquefaction resistance of soils: Journal of Geotechnical and Geoenvironmental Engineering, October 2001, p. 817-833.

SECTION 4: EVALUATION OF EARTHQUAKE-INDUCED LANDSLIDE HAZARD

in the

RICHMOND, MARE ISLAND, AND SAN QUENTIN 7.5-MINUTE QUADRANGLES, CONTRA COSTA COUNTY, CALIFORNIA

by

Jacqueline Bott
P.G. 7459 C.E.G. 2382

Roopl V. Chauhan
P.G. 8754

Marc P. Delattre
P.G. 5230 C.E.G. 1819

Florante G. Perez
P.G. 6972

Michael W Manson
P.G. 3690 C.E.G. 1720

and

David L. Slayter
P.G. 6662

DEPARTMENT OF CONSERVATION
CALIFORNIA GEOLOGICAL SURVEY

Purpose of this Section

This Section of the Seismic Hazard Zone Report presents the analyses and criteria used to delineate of earthquake-induced landslide hazard zones in the Richmond, Mare Island, and San Quentin quadrangles (project area).

ZONING TECHNIQUES

To evaluate earthquake-induced landslide hazard potential in the study area, a method of dynamic slope stability analysis developed by Newmark (1965) was used. The Newmark method as originally implemented analyzes dynamic slope stability by calculating the cumulative down-slope displacement for a given earthquake strong-motion time history. The double integration of the earthquake acceleration recording to derive displacement considers only accelerations above a threshold value that represents the inertial force required to initiate slope movement (Factor of Safety = 1). This threshold value, called the "yield acceleration," is a function of the strength of the earth materials and the slope gradient, and therefore represents the susceptibility of a given area to earthquake-induced slope failure.

As implemented for the preparation of earthquake-induced landslide zones, susceptibility is derived by combining a geologic map modified to reflect material strength estimates with a slope gradient map. Ground motion parameters are calculated using the United States Geological Survey (USGS) National Seismic Hazard Model, and Newmark displacements are estimated from a regression equation developed by Jibson (2007) that uses susceptibility and ground motion parameters. Displacement thresholds that define earthquake-induced hazard zones are from McCrink and Real (1996) and McCrink (2001).

Earthquake-Induced Landslide Susceptibility

Earthquake-induced landslide susceptibility, defined here as Newmark's yield acceleration (1965), is a function of the Factor of Safety (FS) and the slope gradient. To derive a Factor of Safety, an infinite-slope failure model under unsaturated slope conditions was assumed. In addition, material strength is characterized by the angle of internal friction (Φ) and cohesion is ignored. As a result of these simplifying assumptions, the calculation of FS becomes:

$$FS = \frac{\tan \Phi}{\tan \beta}$$

where **β** is the slope gradient. The yield acceleration (a_y) is then calculated from Newmark's equation:

$$a_y = (FS - 1) g \sin \alpha$$

where **FS** is the Factor of Safety, **g** is the acceleration due to gravity, and **α** is the direction of movement of the slide mass, in degrees measured from the horizontal, when displacement is initiated (Newmark, 1965). For an infinite slope failure **α** is the same as the slope gradient angle **(β)**.

These calculations are conducted in an ArcGIS environment by converting the vector (lines, points and polygons) digital geologic map to a raster (regular spaced grid) material strength map that contains the Φ values assigned to the mapped geologic units (Table 1.2). Preparation of a slope gradient (**β**) map is discussed in Section 1.

Ground Motion for Landslide Hazard Assessment

Ground motion calculations used by CGS for regional earthquake-induced landslide zonation assessments are currently based on the USGS probabilistic seismic hazard analysis (PSHA) model for the 2018 Update of the United States National Seismic Hazard Maps (Petersen and others, 2020). The model is set to calculate ground motion hazard in terms of peak horizontal ground acceleration (PGA) at a 10 percent in 50 years exceedance probability level. Raster versions of the PSHA PGA and Modal Magnitude maps for the project area were calculated from the statewide model and applied in the Newmark displacement calculations, as described below. A more detailed description of the development of ground motion parameters used in preparation of the Seismic Hazard Zone for earthquake-induced landslides can be found in Section 2 of this report.

Earthquake-Induced Landslide Hazard Potential

Earthquake-induced landslide hazard potential is derived by combining the susceptibility map (a_y) with the ground motion maps (PGA and Modal Magnitude) to estimate the amount of permanent displacement that a modeled slope might experience. The permanent slope displacement is estimated using a regression equation developed by Jibson (2007). That equation is:

$$\log D_N = -2.710 + \log\left[\left(1 - \frac{a_y}{PGA}\right)^{2.335}\left(\frac{a_y}{PGA}\right)^{-1.478}\right] + 0.424\boldsymbol{M} \pm 0.454$$

where D_N is Newmark displacement and **M** is magnitude. Jibson's (2007) nomenclature for yield acceleration (a_c) and peak ground acceleration (a_{max}) have been replaced here by a_y and PGA, respectively, to be consistent with the nomenclature used in this report.

The above equation was applied using a_y, PGA and Modal Magnitude maps as input, resulting in mean values of Newmark displacement at each grid cell (the standard deviation term at the end of the equation is ignored). The amount of displacement predicted by the Newmark analysis provides an indication of the relative amount of damage that could be caused by earthquake-induced landsliding. Displacements of 30, 15 and 5 cm were used as criteria for rating levels of earthquake-induced landslide hazard potential based on the work of Youd (1980), Wilson and Keefer (1983), and a CGS pilot study for earthquake-induced landslides (McCrink and Real, 1996; McCrink, 2001).

Earthquake-Induced Landslide Zoning Criteria

Seismic Hazard Zones for earthquake-induced landslides were delineated using criteria adopted by the California State Mining and Geology Board (CGS, 2004). Under these criteria, these zones are defined as areas that meet one or both of the following conditions:

1. Areas that have been identified as having experienced landslide movement in the past, including all mappable landslide deposits and source areas as well as any landslide that is known to have been triggered by historic earthquake activity.
2. Areas where the geologic and geotechnical data and analyses indicate that the earth materials may be susceptible to earthquake-induced slope failure.

These conditions are discussed in further detail in the following sections.

Delineation of Earthquake-Induced Landslide Hazard Zones

Upon completion of an earthquake-induced landslide hazard evaluation within a project quadrangle, CGS applies the above criteria to its findings to delineate Earthquake Zones of Required Investigation for earthquake-induced landslides. Based on the evaluation, about 22.3 square kilometers (8.6 square miles) of the quadrangles are included in the Seismic Hazard Zone for earthquake-induced landslides. It encompasses much of the hilly areas of the Berkeley and Richmond hills and the San Pablo Ridge, Sobrante Ridge, and Pinole Ridge, as well as minor unnamed terrain throughout the map area. Following is a description of the criteria-based factors that governed the construction of the Seismic Hazard Zone Map for the project area.

Existing Landslides

Existing landslides typically consist of disrupted soils and rock materials that are generally weaker than adjacent undisturbed rock and soil materials. Previous studies indicate that existing landslides can be reactivated by earthquake movements (Keefer, 1984). Earthquake-triggered movement of existing landslides is most pronounced in steep head scarp areas and at the toe of existing landslide deposits. Although reactivation of deep-seated landslide deposits is less common (Keefer, 1984), a significant number of deep-seated landslide movements have occurred during, or soon after, several recent earthquakes. Based on these observations, all existing landslides with a definite or probable confidence rating are included within the Seismic Hazard Zone. Mapping and categorization of existing landslides is discussed in further detail in Section 1.

Hazard Potential Analysis

Based on the conclusions of a pilot study performed by CGS (McCrink and Real, 1996; McCrink, 2001), the Seismic Hazard Zone for earthquake-induced landslides encompass all areas that have calculated Newmark displacements of 5 centimeters or greater.

ACKNOWLEDGMENTS

The authors thank the following individuals and organizations for their assistance in obtaining the data necessary to complete this project: Chris Castanchoa and Yader Bermudez of the City of Richmond, Jamie Aldred of the City of Pinole, Darwin Myers of Contra Costa County, and Jeff Balantine of the City of El Cerrito for review comments. At CGS, Alexa Evans and Daniel Langermann assisted with geotechnical data collection and entry efforts. Bob Moskovitz and Jonathan Goergen provided database compilation and analysis support. Kate Thomas and Michael Falsetto prepared the final Seismic Hazard Zone Map and prepared the graphic displays for this report. Tim Dawson and Erik Frost provided technical review for this report.

REFERENCES

California Geological Survey, 2004, Recommended criteria for delineating seismic hazard zones in California: California Geological Survey Special Publication 118, 12 p., originally published 1992, available on-line at: http://www.conservation.ca.gov/cgs/publications/sp118..

Jibson, R.W., 2007, Regression models for estimating coseismic landslide displacement: Engineering Geology, vol. 91, issue 2-4, p. 209-218.

Keefer, D.K., 1984, Landslides caused by earthquakes: Geological Society of America Bulletin, v. 95, no. 4, p. 406-421.

McCrink, T.P., 2001, Mapping earthquake-induced landslide hazards in Santa Cruz County *in* Ferriz, H., and Anderson, R., *editors*, Engineering geology practice in northern California: California Geological Survey Bulletin 210 / Association of Engineering Geologists Special Publication 12, p. 77-94.

McCrink, T.P., and Real, C.R., 1996, Evaluation of the Newmark method for mapping earthquake-induced landslide hazards in the Laurel 7.5-minute Quadrangle, Santa Cruz County, California: California Division of Mines and Geology Final Technical Report for U.S. Geological Survey Contract 143-93-G-2334, U.S. Geological Survey, Reston, Virginia, 31 p.

Newmark, N.M., 1965, Effects of earthquakes on dams and embankments: Geotechnique, v. 15, no. 2, p. 139-160.

Petersen, M.D., Shumway, A.M., Powers, P.M., Mueller, C.S., Haller, K.M., Moschetti, M.P, Frankel, A.D., Rezaeian, S., McNamara, D.E., Luco, N., Boyd, O.S., Rukstales, K.S., Jaiswal, K.S., Thompson, E.M., Hoover, S.M., Clayton, B.S., Field, E.H., and Zeng, Y., 2020, The 2018 updated of the US National Seismic Hazard Model: Overview of model and implications: Earthquake Spectra, vol. 36, no. 1, p. 5–41, doi: 10.1177/8755293019878199.

Quantum Spatial, Inc., 2019, Northern California 3DEP QL1 QL2 LiDAR Project Report, report submitted to USGS under contract # G16PC00016.

U.S. Geological Survey, 2005, Digital Surface and Terrain Models (DSM, DTM), lidar-derived digital terrain model for Contra Costa County: https://catalog.data.gov/dataset/digital-surface-and-terrain-models-dsmdtm-lidar-derived-digital-terrain-model-for-san-mateo-couc2700

Wilson, R.C., and Keefer, D.K., 1983, Dynamic analysis of a slope failure from the 1979 Coyote Lake, California, earthquake: Bulletin of the Seismological Society of America, v. 73, p. 863-877

Youd, T.L., 1980, Ground failure displacement and earthquake damage to buildings: American Society of Civil Engineers Conference on Civil Engineering and Nuclear Power, 2d, Knoxville, Tennessee, 1980, v. 2, p. 7-6-2 to 7-6-26.

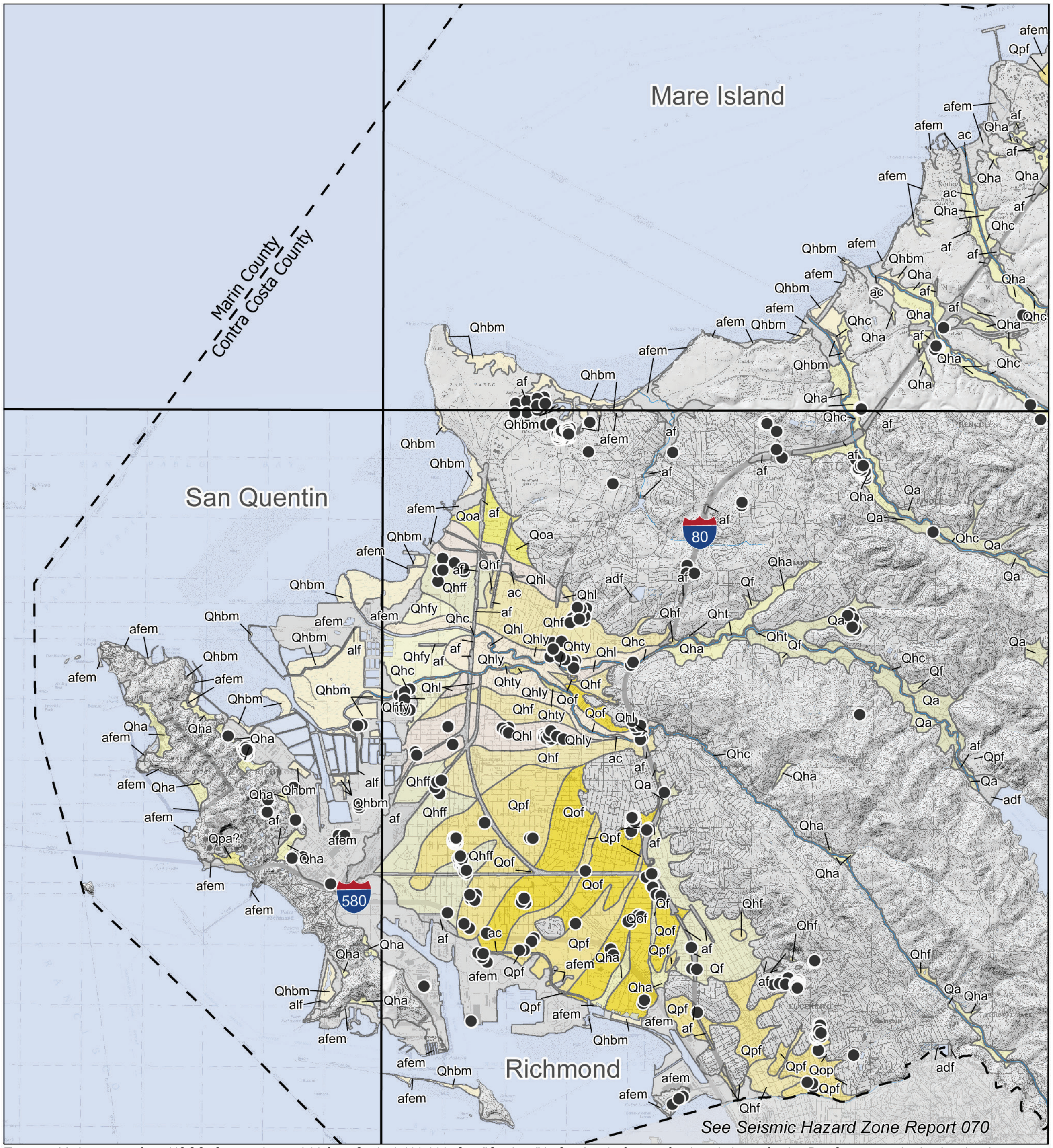

Topographic base map from USGS. Contour interval 20 feet. Scale 1:100,000. See "Geology" in Section 1 of report for descriptions of units. Pre-Quaternary bedrock units shown without color. Map preparation by Michael Falsetto, CGS.

SAN QUENTIN, MARE ISLAND, AND RICHMOND QUADRANGLES

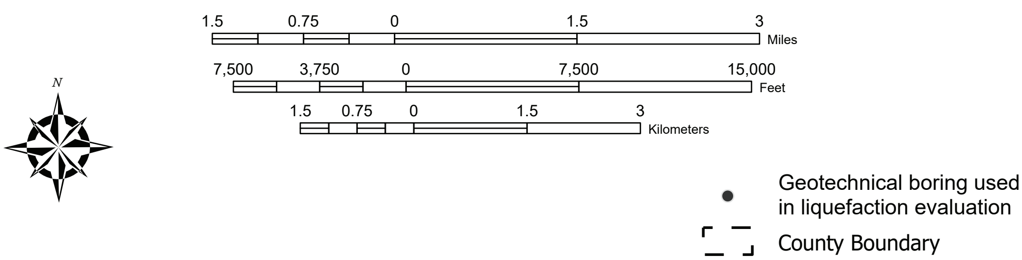

Plate 1.1 Quaternary geologic materials and borehole locations used to evaluate areas susceptible to earthquake-induced liquefaction in the study area.

Topographic base map from USGS. Contour interval 20 feet. Scale 1:100,000. See "Geology" in Section 1 of report for descriptions of units. Map preparation by Michael Falsetto CGS.

SAN QUENTIN, MARE ISLAND, AND RICHMOND QUADRANGLES

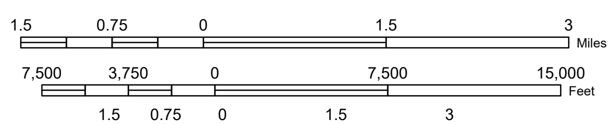

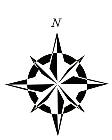

- Shear test sample location
- GSI measurement location
- Landslide
- County Boundary

Plate 1.2 Geologic materials, landslide inventory, shear test sample locations, and Geologic Strength Index (GSI) measurement locations used in evaluating earthquake-induced landslide hazard in the study area.

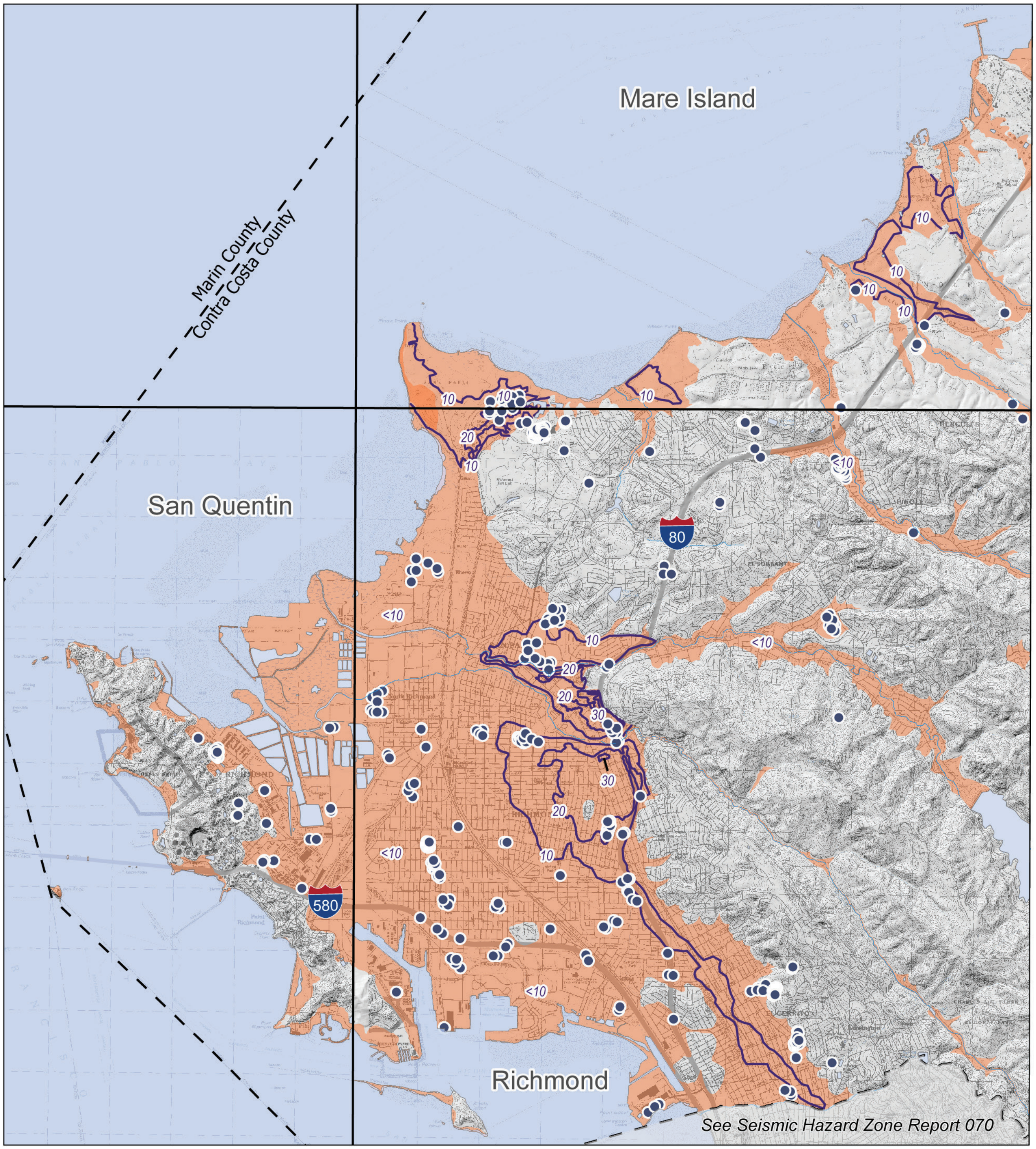

Topographic base map from USGS. Contour interval 20 feet. Scale 1:100,000. Map preparation by Michael Falsetto CGS.

SAN QUENTIN, MARE ISLAND, AND RICHMOND QUADRANGLES

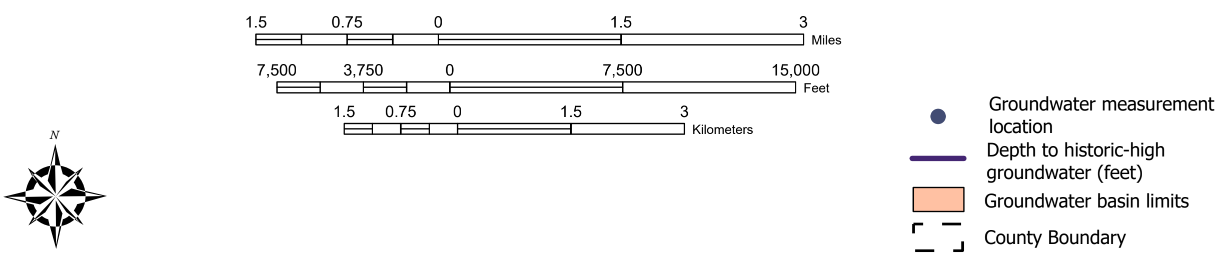

Plate 1.3 Groundwater basins and groundwater measurement points used to determine depth to historic high groundwater contours in the study area.

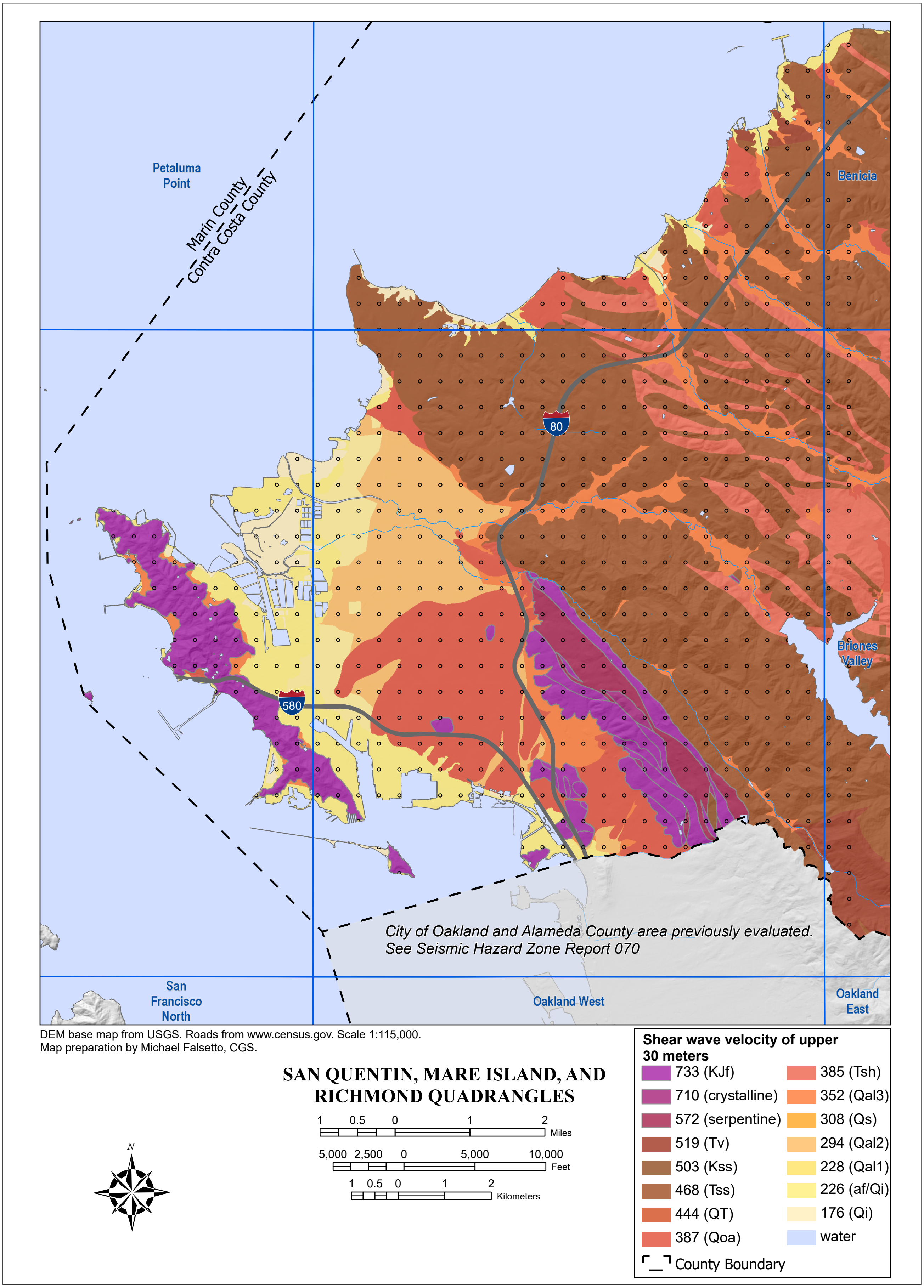

Plate 2.1 V_{S30} groups and corresponding geologic units extracted from the state-wide V_{S30} map developed by Wills and others (2015), for evaluating seismic hazards in the study area.

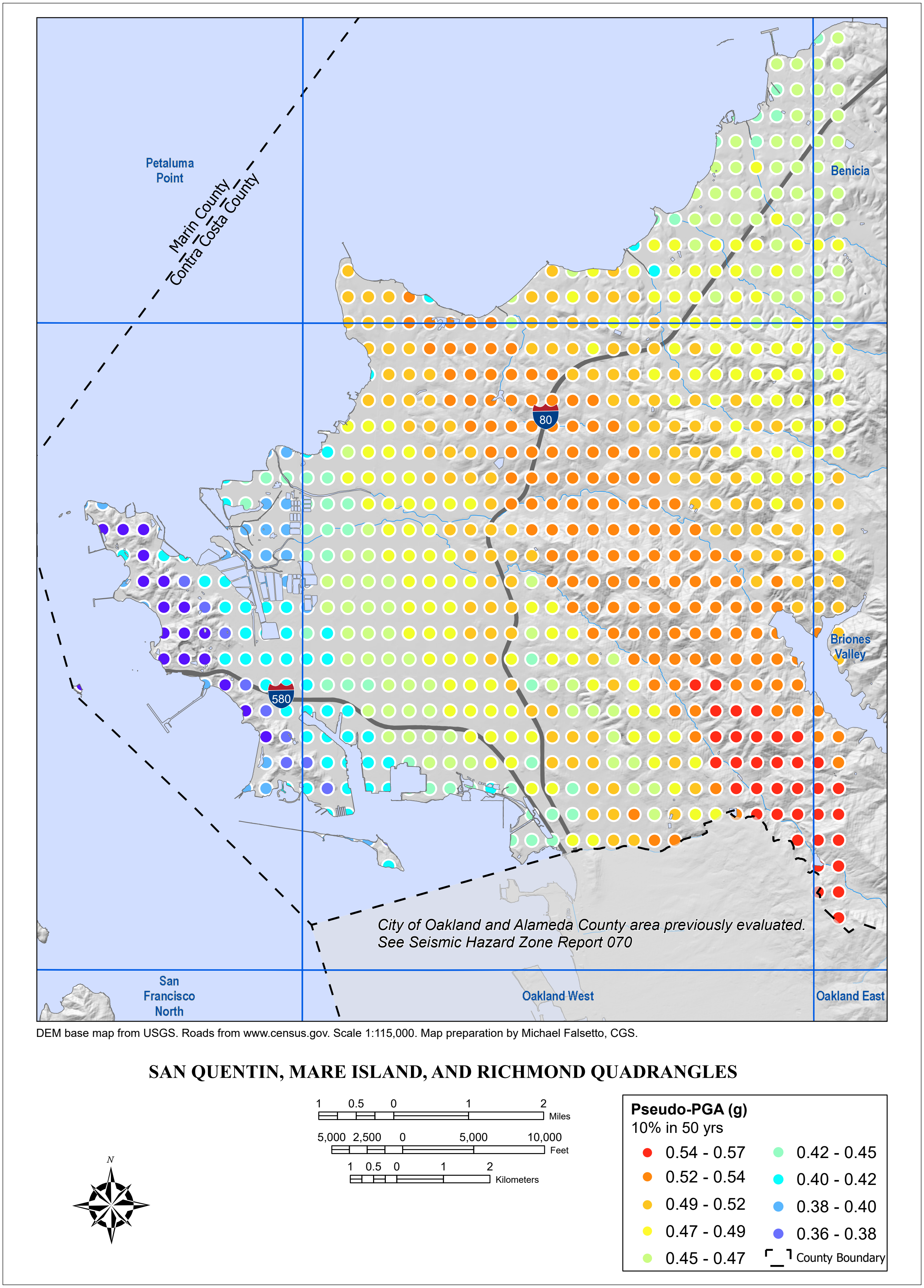

Plate 2.2 Pseudo-PGA for evaluating seismic hazards in the study area.

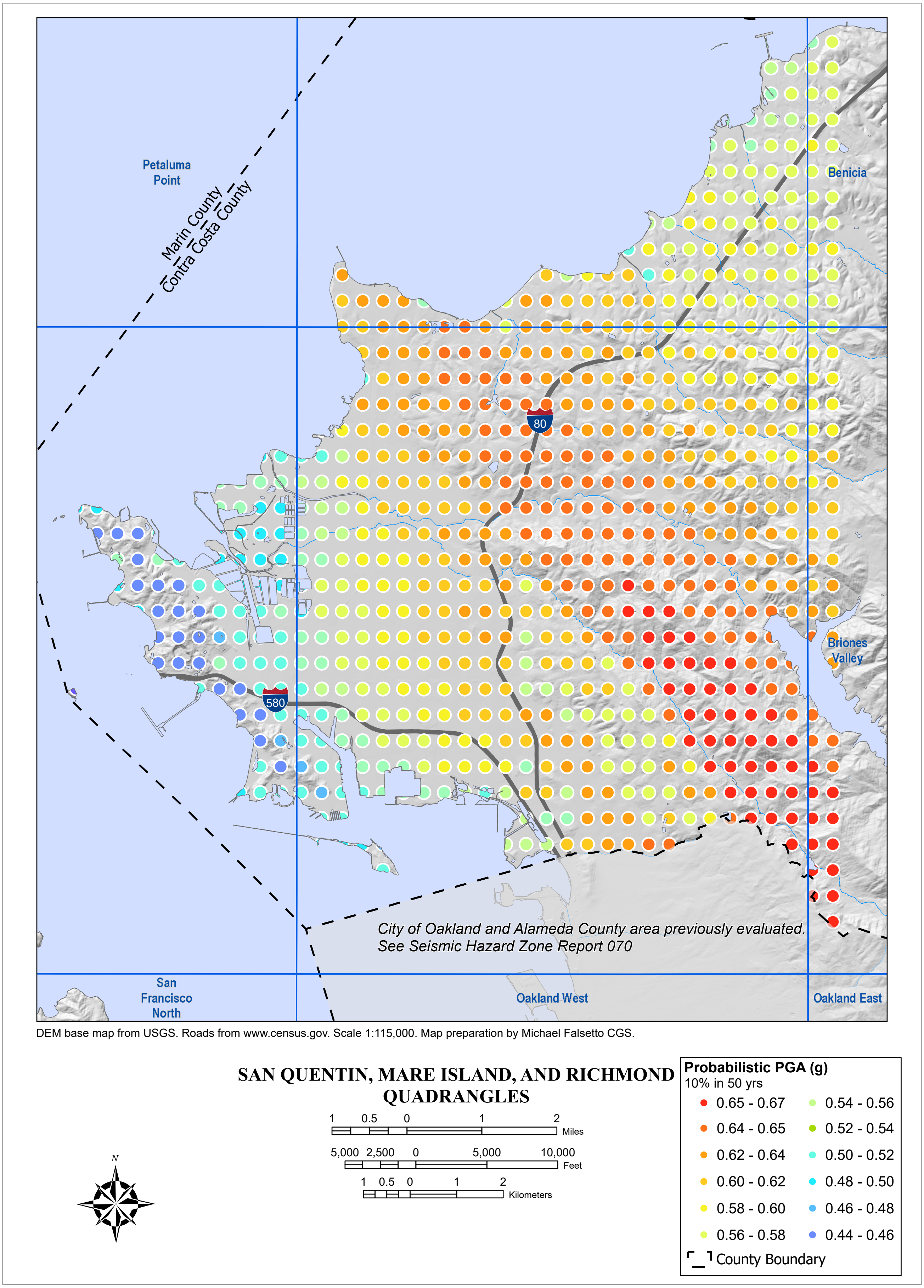

Plate 2.3 Probabilistic peak ground acceleration for evaluating seismic hazards in the study area.

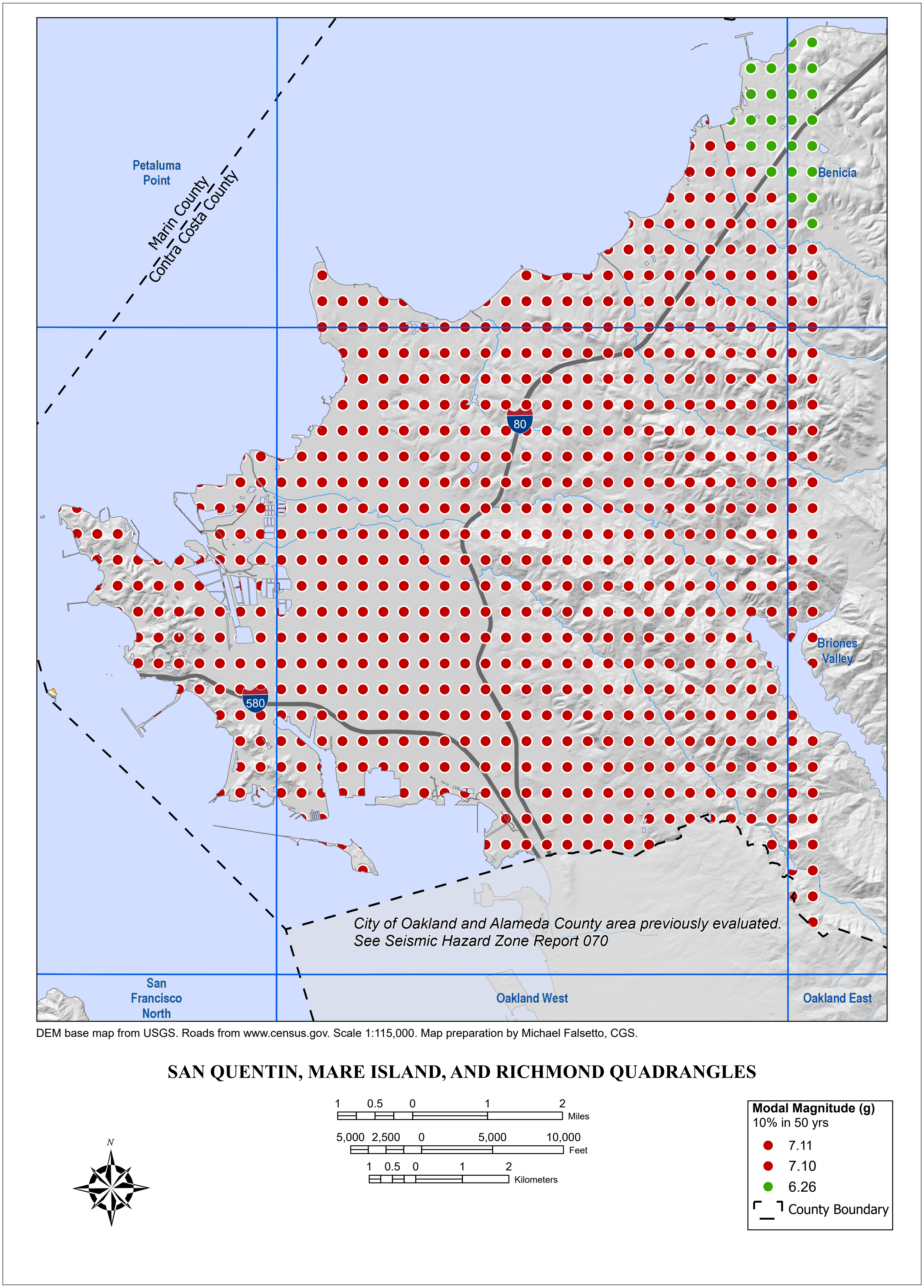

Plate 2.4 Modal magnitude for evaluating seismic hazards in the study area

AUTHORSHIP CREDITS

PUBLICATION TITLE: SEISMIC HAZARD ZONE REPORT 134 FOR THE RICHMOND, MARE ISLAND, AND SAN QUENTIN 7.5-MINUTE QUADRANGLES, CONTRA COSTA COUNTY, CALIFORNIA

Lead Author – Jacqueline Bott, Engineering Geologist

CERTIFIED ENGINEERING GEOLOGIST
Jacqueline Bott
No. 2382
STATE OF CALIFORNIA

Date: February 22, 2024

Work in Responsible Charge: : Geologic and geotechnical data acquisition, interpretation, and analysis; geologic mapping; digital imagery and elevation data analysis; field verification; liquefaction/landslide modeling; and final seismic hazard zone map production.

Section Author – Rui Chen, Professional Geologist

PROFESSIONAL GEOLOGIST
Rui Chen
No. 8598
STATE OF CALIFORNIA

Date: February 22, 2024

Work in Responsible Charge: Probabilistic ground motion hazard assessment.

Project Manager – Erik Frost, Senior Engineering Geologist

CERTIFIED ENGINEERING GEOLOGIST
Erik K. Frost
No. 2704
STATE OF CALIFORNIA

Date: February 22, 2024

Work in Responsible Charge: Validation of mapping process and pre-release seismic hazard zone report review

Program Manager – Timothy Dawson, Supervising Engineering Geologist

CERTIFIED ENGINEERING GEOLOGIST
Timothy E. Dawson
No. 2618
STATE OF CALIFORNIA

Date: February 22, 2024

Work in Responsible Charge: Technical review and approval.